Geochemistry, Geophysics, Geosystems

RESEARCH ARTICLE
10.1029/2022GC010610

Key Points:

- New seismic waveform tomography images a continuous low-velocity anomaly beneath East Africa-Arabia interpreted as an extant plume head
- The body of partially molten rock is shaped as a 3-pointed star by the lithosphere-asthenosphere boundary and underlies all the intraplate volcanic areas
- Complex star-shaped plume heads spreading via thin-lithosphere valleys can explain the dispersed, protracted volcanism in many ancient large igneous provinces

Supporting Information:

Supporting Information may be found in the online version of this article.

Correspondence to:

C. Civiero,
cciviero@cp.dias.ie

Citation:

Civiero, C., Lebedev, S., & Celli, N. L. (2022). A complex mantle plume head below East Africa-Arabia shaped by the lithosphere-asthenosphere boundary topography. *Geochemistry, Geophysics, Geosystems*, *23*, e2022GC010610. https://doi.org/10.1029/2022GC010610

Received 11 JUL 2022
Accepted 7 OCT 2022

A Complex Mantle Plume Head Below East Africa-Arabia Shaped by the Lithosphere-Asthenosphere Boundary Topography

Chiara Civiero[1,2], Sergei Lebedev[1,3], and Nicolas L. Celli[1]

[1]Dublin Institute for Advanced Studies, Geophysics Section, Dublin, Ireland, [2]Institut de Ciències del Mar, ICM-CSIC, Barcelona, Spain, [3]Bullard Laboratories, Department of Earth Sciences, University of Cambridge, Cambridge, UK

Abstract Hot plumes rising from Earth's deep mantle are thought to cause uplift, rifting and large igneous province (LIP) emplacement. LIP volcanism in continents often spans tens of Ma and scatters unevenly over broad areas. This has been attributed to lateral flow of hot plume material, but observational evidence on such flow is scarce. New waveform tomography with massive data sets reveals detailed seismic velocity structure beneath the East Africa-Arabia region, where these processes occur at present. It shows interconnected sub-lithospheric corridors of hot, partially molten rock, fed by three mantle upwellings beneath Kenya, Afar, and Levant. The spatio-temporal distribution of the volcanism suggests that we are witnessing an integral plume head, which morphed into a three-pointed star by ponding and channeling within thin-lithosphere corridors. Plate reconstructions indicate that it spread south-to-north since ~45 Ma. These results suggest that complex-shape plume heads can explain the enigmatic, scattered LIP volcanism and are, probably, an inherent feature of plume-continent interaction.

1. Introduction

1.1. Overview

Mantle plumes, the thermo-chemical instabilities rising from the Earth's core-mantle boundary are believed to be the primary cause of the emplacement of Large Igneous Provinces (LIPs) (Morgan, 1971, 1972; Richards et al., 1989). The term "plume head" is often applied to the leading portion of a plume, rising through the Earth's deep mantle. Some of the early conceptual models and experiments pictured a large, round head of a plume, followed by a narrow tail (e.g., Campbell & Griffiths, 1990; Richards et al., 1989). Other laboratory experiments and numerical models show complex and variable shapes of the upwellings (e.g., Davaille, 1999; Farnetani & Samuel, 2005; Koppers et al., 2021). Mantle structure, including the partial barrier to convection at the 660-km discontinuity and thermo-chemical heterogeneities elsewhere may strongly affect the morphology of the upwellings (Bercovici & Mahoney, 1994; Courtillot et al., 2003; Cserepes & Yuen, 2000; Koppers et al., 2021).

Once the plume reaches the bottom of the lithosphere, the hot material must accumulate below the lithosphere-asthenosphere boundary (LAB) and spread laterally. Morgan (1971, 1972) postulated that horizontal currents in the asthenosphere flow radially away from the plume center. R. White and McKenzie (1989) proposed that a narrow (150-km diameter) hot plume rising from the deep mantle is deflected laterally by the overlying plate to form a circular, mushroom-shaped head of anomalously hot mantle, 1,000–2,000 km in diameter (Figure 1a). They proposed that the lithosphere can be rifted anywhere above this mushroom-shaped head, and voluminous intraplate volcanism is produced by the decompression melting of the upwelling hot asthenosphere. In this paper, we also apply the term "plume head" to these accumulations of hot material below the LAB.

Continental lithosphere shows strong lateral variations in its thickness (e.g., Fullea et al., 2021). Influenced by the LAB topography, plume heads below the lithosphere may develop in asymmetric, complex shapes (e.g., Burov & Gerya, 2014; Burov et al., 2007; Camp, 1995). Sleep (1997) investigated the probable ponding of the buoyant plume-head material beneath thin-lithosphere areas and its drainage patterns, determined by pre-existing lithospheric thickness variations and the evolution of new thin-lithosphere channels due to rifting and seafloor spreading. Plume material has been proposed to sometimes flow for hundreds of kilometers below the lithosphere, guided by thin-lithosphere corridors (Ebinger & Sleep, 1998; Steinberger et al., 2019), and such flow could explain scattered volcanism. The broad distributions of LIP volcanism (e.g., Bryan & Ernst, 2008) have fueled debate on how plume heads interact with the lithosphere and on the basic mechanisms of the volcanism

Geochemistry, Geophysics, Geosystems 10.1029/2022GC010610

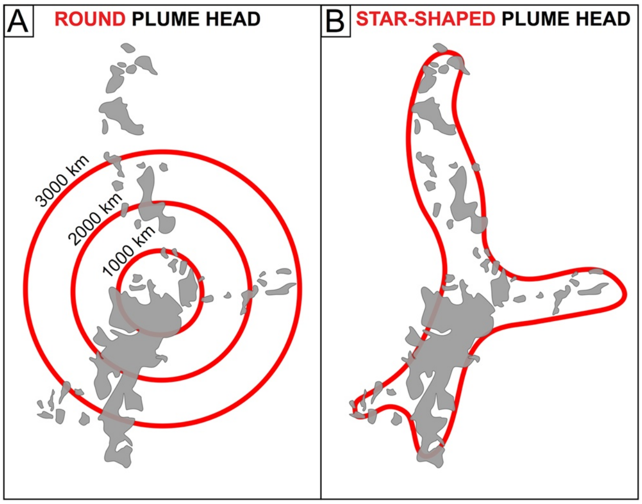

Figure 1. Alternative models of the mantle plume head beneath a continent. (a) The conventional view of a circular plume head (R. White & McKenzie, 1989) with different hypothetical diameters. The distributions of large igneous province volcanism are not matched by the circular shape. (b) A plume head shaped as a three-pointed star, morphed into the shape by the topography of the lithosphere-asthenosphere boundary. A body of hot, partially molten rock is observed to fill this shape beneath the East Africa-Arabia region, closely matching the distribution of the volcanism at the surface.

(e.g., Ballmer et al., 2015; Foulger, 2007). Peace et al. (2020), for example, reviewed the LIPs associated with the Pangaea break-up, argued that the spatial distribution of the volcanism is inconsistent with the standard plume view and suggested that the plume origin must be ruled out as the cause altogether.

The East Africa-Arabia region displays spectacular signs of an ongoing mantle-plume impact onto its continental lithosphere (Figure 2). The East African Rift System (EARS) extends over 2,000 km from the Red Sea in the north to Mozambique in the south. It encompasses two regions of topographic uplift, the Ethiopian and the Kenyan Domes, which rise over 2 km high (Ebinger et al., 1989). A zone of NW-SE extension, the Turkana Depression, developed in the Early Cretaceous and lies in between these domes. Whereas the Ethiopian Dome is cut by a single rift system, the Kenyan Dome is cut by two rifts, the Eastern (or Gregory) rift and the Western rift, separated by the cold, mechanically strong lithosphere of the Tanzania craton (Chorowicz, 2005). In the Arabian Plate, other two broad, undulating swells, the West Arabian Swell, and the East Anatolian Plateau to the north stand at 1.5–2 km elevation (Bohannon et al., 1989; Şengör et al., 2003). Rifting and continental breakup occur at the EARS, Red Sea, and Gulf of Aden, radiating from the Afar rift-rift-rift triple junction where the Arabian, Nubian, and Somalian Plates meet (e.g., Corti, 2009; Ebinger & Casey, 2001; Wolfenden et al., 2004). Continental rifting initiated at ∼35 Ma in the Gulf of Aden and at ∼28 Ma in the Red Sea (e.g., Wolfenden et al., 2005). The earliest extension recorded in the EARS occurred west of the present-day Lake Turkana at ∼25 Ma, within lithosphere stretched during a Mesozoic rifting event (e.g., Hendrie et al., 1994). Extension between the Nubian and Somalian Plates initiated in the southern and central Main Ethiopian Rift at ∼18 Ma (Wolfenden et al., 2004).

Diffuse basaltic volcanism started in southern Ethiopia/northern Turkana ∼45 Ma ("Eocene Initial Phase" according to Rooney, 2017), and propagated, gradually, to Tanzania and northward to western Arabia (Figures 2b and 2c, see Text S1 and Table S1 in Supporting Information S1 for further details). The velocity of the African plate is not constant (P. G. Silver et al., 1998), thus the progression of volcanism may be further controlled by the uneven NE plate motion. Along the eastern Mediterranean coast, the volcanism started in the Levant region ∼26 Ma and propagated northward to eastern Anatolia and southward to western Arabia (e.g., Al Kwatli et al., 2012; Krienitz et al., 2009). Once initiated, volcanism at most locations has continued until present, for millions of years, in contrast with the short-lived, age-progressive volcanism that usually forms the OIB chains. Magmatic intrusions were facilitated by the extensional regime, weakening the lithosphere that continued to fail along the original fractures when undergoing to further extensional stresses (Bastow & Keir, 2011; Rogers, 2006; Rooney, 2010).

In this study, we use seismic waveform tomography to show that a continuous low-seismic-velocity anomaly, shaped as a three-pointed star, extends beneath all the areas of the Cenozoic intraplate volcanism in the East Africa-Arabia region (Figure 1b). Our results suggest that the imaged low-velocity anomaly is the seismic expression of a large volume of plume material morphed into a star shape by the topography of the LAB and captured by the thin-lithosphere valleys, which allow it to flow thousands of kilometers across. This plume material—which we consider as the extant East Africa-Arabia plume head—is fed by the continuing supply of hot material through thin stems below it and has evolved for millions and tens of millions years. We also compare the tomography with previously published tomographic models and other geophysical, geochemical and geological data to discuss the origin of the mantle upwellings below the region and their role in the evolution of the system.

1.2. Previous Studies on the Mantle Upwellings Beneath East Africa-Arabia

The uplift, rifting, and volcanism in the East Africa-Arabia region have been attributed to one or more plumes, based on geochemical, seismic, and other evidence (Camp & Roobol, 1992; Chang et al., 2020; Ebinger

10.1029/2022GC010610

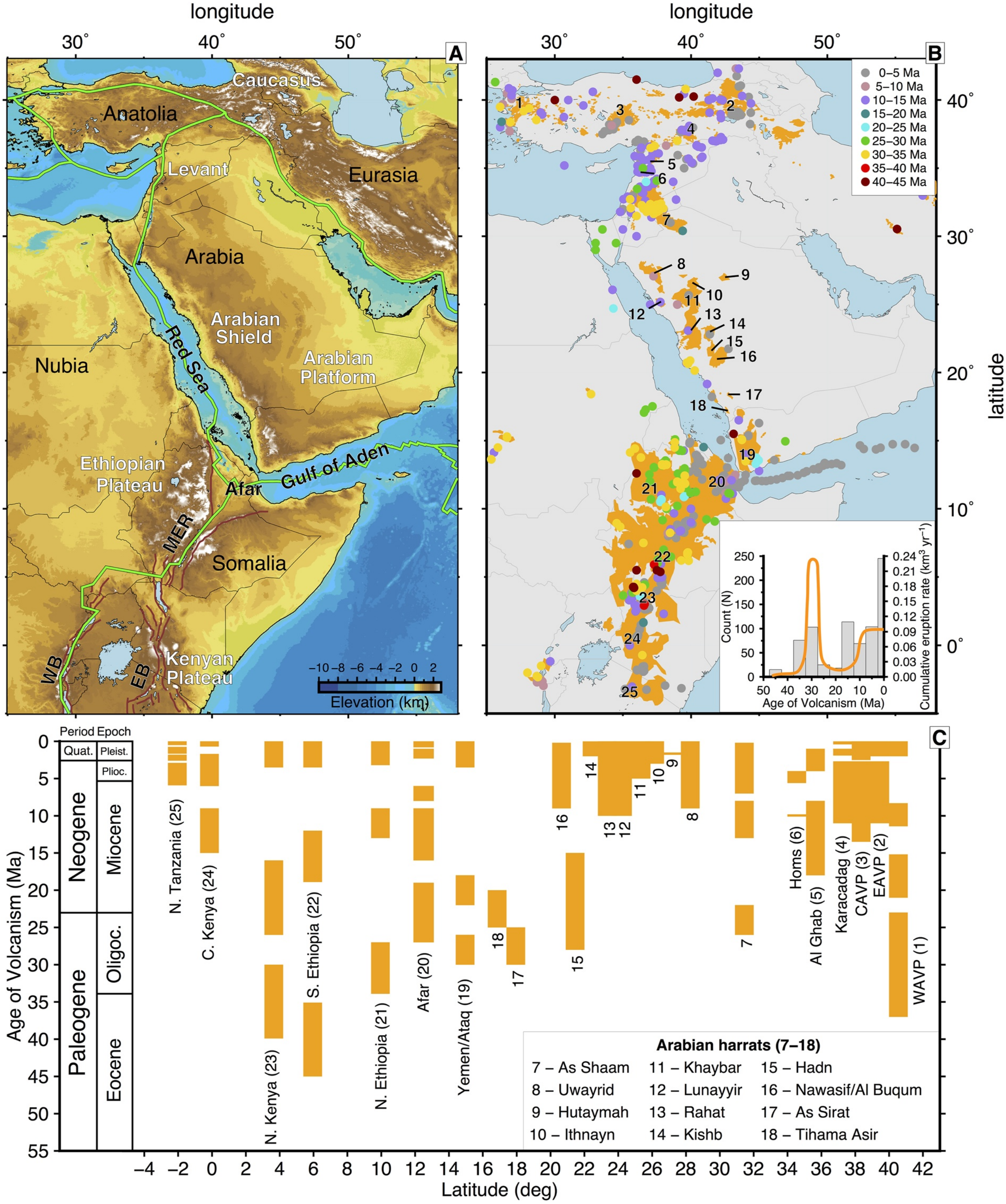

Figure 2. Topography and volcanism of the East Africa-Arabia system. (a) Topography and main tectonic features. Plate boundaries: green lines. WB and EB: Western and Eastern Branches of the East African Rift; MER: the Main Ethiopian Rift. (b) Intraplate basaltic volcanism in the region. The volcanic fields are plotted in orange. Each number indicates a volcanic area. Published volcanic samples from the earthchem.org database, classified as basalt and dated using mainly noble gases and radiogenic isotopes, are shown as color-coded filled circles. Inset: histogram showing the ages of the 776 available dated samples in 5-Ma bins and the cumulative eruption rate (orange curve) for the main East African volcanic sites (Ebinger et al., 1993; George et al., 1998; Rooney, 2017). (c) Age-latitude plot of the igneous activity plotted in panel (b), from Tanzania in the south to Anatolia in the north. For the data compilation, see Table S1, Text S1, and Text S2 in Supporting Information S1.

et al., 1989; Fishwick & Bastow, 2011; Montelli et al., 2006; Nelson et al., 2012). Thin-lithosphere corridors have been proposed to channel the flow of plume material to volcanic fields hundreds of kilometers away (Camp & Roobol, 1992; Ebinger & Sleep, 1998; Faccenna et al., 2013).

The strongest geochemical evidence supporting the presence of plume material below the region is the lack of a prominent contribution from shallow, depleted MORB mantle in the source material for pre-rift volcanism (Baker et al., 1996; Furman et al., 2006; Kieffer et al., 2004). If this episode of volcanism were not plume-related, passive rifting would have allowed the shallow mantle source to dominate in the geochemistry of the mafic lavas (Nelson et al., 2012). Isotopic measurements in the basalts of southern Ethiopia and Kenya, however, are significantly distinct from those in Afar (e.g., Furman et al., 2006; George et al., 1998; Nelson et al., 2012) and those in Levant (Krienitz et al., 2009), even though all indicate deep-mantle reservoirs, with a lithospheric component. Considered together, the variable compositional signatures of the rocks are consistent with the occurrence of at least two upwelling sources of volcanism below the African plate and cast doubt on the hypothesis that all the magmatism was caused by one plume alone (Pik et al., 2006).

The inference that the volcanism is fed by different mantle upwellings is corroborated by several tomography models (Boyce et al., 2021; Chang et al., 2020; Chang & Van der Lee, 2011; Montelli et al., 2006; Tsekhmistrenko et al., 2021), showing separate low-velocity anomalies in the lower mantle, attributable to multiple plumes. Seismic tomography maps the distribution of seismic velocity anomalies and, by inference, thermal anomalies in the mantle (as well as compositional heterogeneity and, particularly in hot-asthenosphere and thin-lithosphere regions, partial melting), but tomography studies in the region to date have yielded little agreement in models and interpretations. A broad low-velocity anomaly has been imaged in the deep lower mantle beneath southern Africa, tilting northeastward at shallower lower-mantle depths (Nyblade & Robinson, 1994; Ritsema et al., 1999). The inferred "African Superplume" was proposed as the primary source of volcanism throughout East Africa-Arabia (e.g., Hansen et al., 2012). Some regional tomographic studies show adjacent low-velocity structures beneath East Africa and Arabia (e.g., Debayle et al., 2001; Montagner et al., 2007; Sicilia et al., 2008), whereas other models image isolated low-velocity anomalies below Ethiopia and Kenya (Bastow et al., 2008; Chang et al., 2015; Emry et al., 2019; Montelli et al., 2006), and a possible third beneath Arabia (Koulakov et al., 2016) or Jordan (Chang & Van der Lee, 2011).

A channel of hot material from Afar has been proposed to extend laterally below Arabia and the Red Sea coast (Camp & Roobol, 1992; Ebinger & Sleep, 1998). Some tomography models show a broad, low-velocity feature in the upper mantle extending from the Red Sea into the interior of Arabia (Benoit et al., 2003; Debayle et al., 2001; Emry et al., 2019; Fishwick, 2010) and, more recently, a narrow anomaly aligned with the Red Sea but offset to the east (Chang & Van der Lee, 2011; Chang et al., 2011; Koulakov et al., 2016; Lim et al., 2020; Tang et al., 2018; Yao et al., 2017). Low shear-wave velocities beneath the Gulf of Aden down to ∼150 km depth were also reported, suggesting that the plume below Afar may be feeding the Gulf of Aden ridge (Sicilia et al., 2008). The strong differences between the tomographic models are, in large part, due to the relatively sparse data sampling of the region, especially until recently.

2. Waveform Tomography

Starting with the recently published model AF2019 (Celli, Lebedev, Schaeffer, & Gaina, 2020), we extend it northward to Anatolia. The model was computed using all freely available (at the time of data retrieval) broadband data in the region, combined with global data to create a very dense sampling of the region and maximize the imaging resolution (Figure 3). The broadband data were downloaded from the following data centers: the Incorporated Research Institutions for Seismology (IRIS; http://www.iris.edu), the GEOFON Global Seismic Network (https://geofon.gfz-potsdam.de), the Observatories and Research Facilities for European Seismology (ORFEUS; http://www.orfeus-eu.org), the French Seismologic and Geodetic Network Résif (RESIF; https://www.resif.fr), the National Observatory of Athens (NOA; http://bbnet.gein.noa.gr), the Kandilli Observatory and Earthquake Research Institute (KOERI; http://www.koeri.boun.edu.tr), and the Instituto Nazionale di Geofisica e Volcanologia (INGV; https://www.ingv.it).

The global waveform data set contains recordings at 6,360 seismic stations in total, and around 400 seismic stations are situated in the East Africa-Arabia region (Figure 3). Station information, including the seismic experiment and data center, can be found Table S2 in Supporting Information S1. We selected all earthquakes (27,550

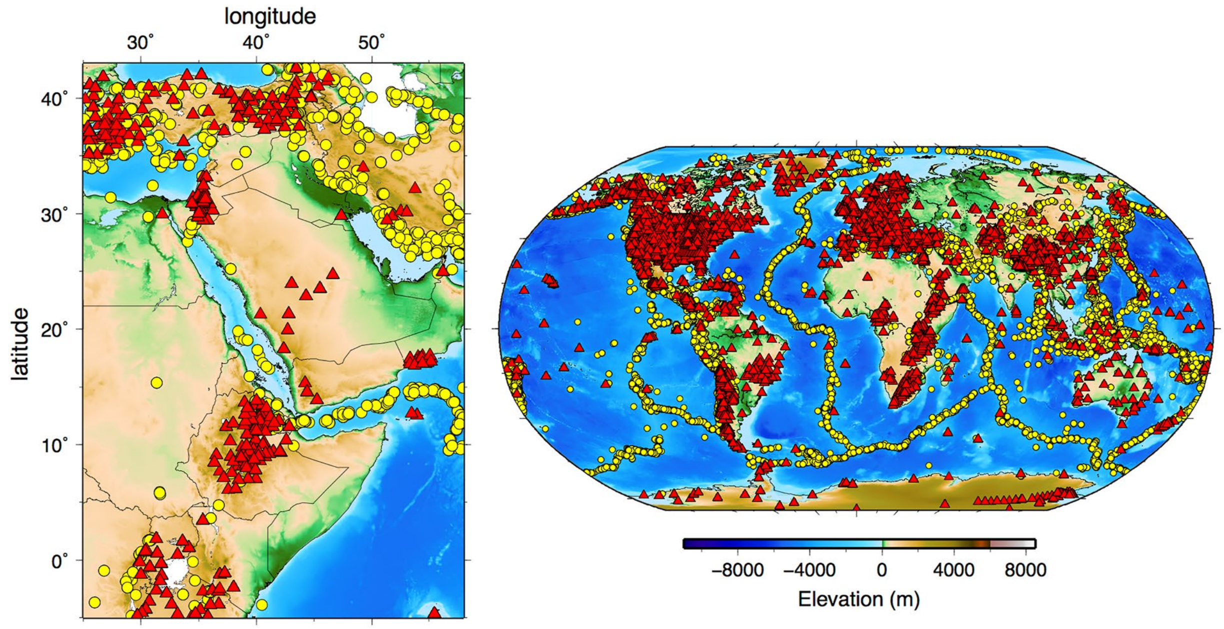

Figure 3. Earthquakes and seismic stations used in our seismic tomography. Left: Earthquakes and seismic stations within the study area (see Table S2 in Supporting Information S1 for details on the seismic networks, arrays and experiments). Right: Earthquakes and seismic stations around the globe. Events are plotted as yellow circles, broadband seismic stations as red triangles.

in total) with magnitude over 4.5 from the Harvard Centroid Moment Tensor Solutions catalog (Dziewonski et al., 1981; Ekström et al., 2012) since 1994. Waveform inversion was performed to extract structural information from surface, S and multiple S waves in over 1.2 million vertical-component global and regional seismograms. Our model is focused on East Africa-Arabia, with the data coverage in this region maximized (all freely available broadband data were included) and the regularization tuned to optimize the resolution in this specific area. The global data complements the regional data set and ensures dense sampling of the entire region.

The inversion procedure used to obtain the S-wave model was split into three steps. We began by applying the Automated Multimode Inversion (AMI; Lebedev et al., 2005), which performs automated, accurate processing of large numbers of broadband seismograms. The result of the waveform inversion of each seismogram is a set of linear equations with uncorrelated uncertainties (Nolet, 1990) describing 1D average P- and S-wave velocity perturbations within the sensitivity volumes between the source and receiver with respect to a 3D reference model (Lebedev & Van Der Hilst, 2008). In the crust, we used the 3D model CRUST2 (Bassin et al., 2000) smoothed across cell boundaries, and augmented with added topography and bathymetry databases (Lebedev and Van Der Hilst, 2008). The mantle reference model for tomography is the global average profile (Lebedev and Van Der Hilst, 2008). Perturbations in both the crust and in the mantle are solved for, resolving the crust-mantle trade-offs and preventing artifacts in the mantle due to unaccounted-for crustal structure (Schaeffer & Lebedev, 2014).

In the second step, all the equations produced by AMI were solved together for the 3D distributions of P and S wavespeeds and the azimuthal anisotropy of the S-wave speed, subject to smoothing and slight norm damping. The model is parameterized using a triangular grid (Wang & Dahlen, 1995) with an average 327-km interknot spacing and a depth parameterization over 18 and 10 depth nodes for S-and P-wave velocities, respectively (S-wave velocities: 7, 20, 36, 56, 80, 110, 150, 200, 260, 330, 410−, 410+, 485, 585, 660−, 660+, 809, and 1,007 km; P-wave velocities: 7, 20, 36, 60, 90, 150, 240, 350, 485, and 585 km). Rayleigh-wave speeds are sensitive primarily to S-wave velocities, but their sensitivity to P-wave velocities is also not negligible. P-velocity perturbations, however, cannot be resolved independently from S-velocity ones with Rayleigh-wave data. We damped the difference between P- and scaled S-velocity perturbations (Lebedev & Van Der Hilst, 2008), which gave the inversion more flexibility than imposing a rigid ratio. The P- and S-velocity images are still similar, and we present only the latter. We also inverted for S-wave 2Ψ azimuthal anisotropy in order to prevent anisotropic heterogeneities from mapping into isotropic ones.

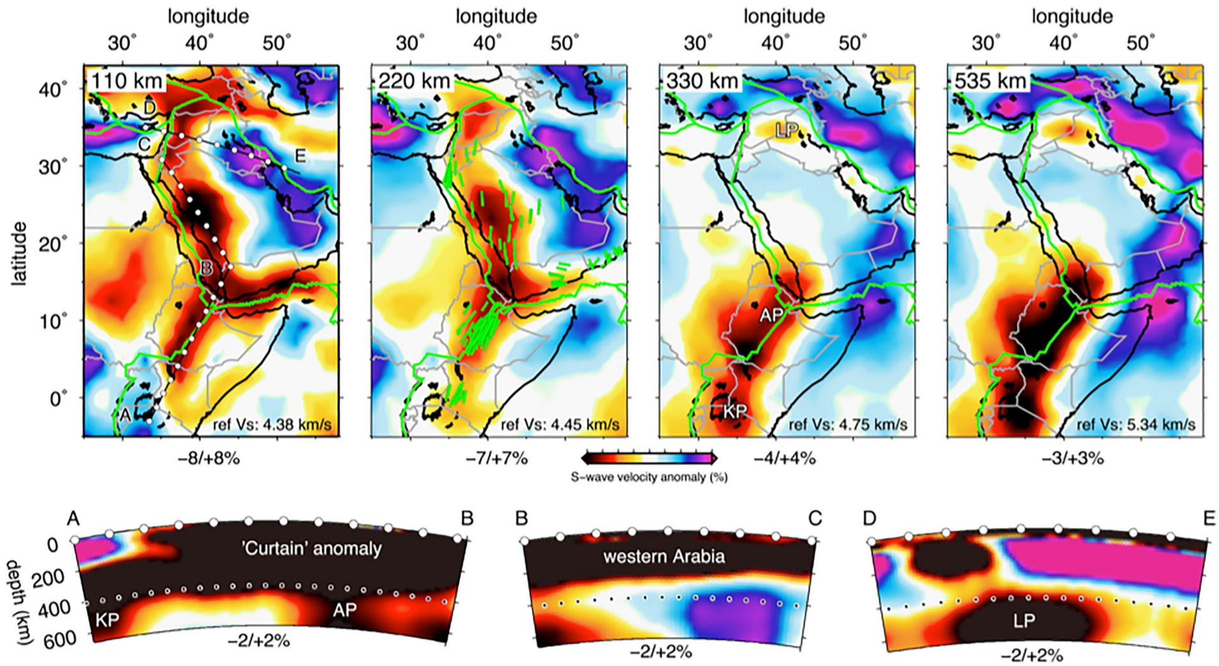

Figure 4. Shear-wave tomography model. Top: Depth slices at four upper-mantle depths. SKS splitting measurements (from the compilation in Gao et al. (2010)) are plotted as green bars in the 200-km-depth map. A more complete compilation of the measurements is shown Figure S6 in Supporting Information S1. Plate boundaries: green lines. AP: Afar Plume; KP: Kenya Plume; LP: Levant Plume. Bottom: cross-sections through key low-velocity features. Section AB is along the "curtain" low-velocity anomaly beneath EARS, BC—along the low-velocity channel below the Arabian Shield, DE—through the Levant Plume (LP). The locations of the profiles are indicated in the 110-km-depth map, with the white-circle spacing of 2°. Dotted line in the cross-sections: 410-km discontinuity.

In the final step of the inversion procedure, we exploited the data set redundancy and selected only the most mutually consistent data through a posteriori outlier analysis. From a first-iteration model, we computed the synthetic data by multiplication of the sensitivity matrix and the model vector. We then compared the synthetic and real data and discarded the ones with the largest misfits, due mostly to earthquake mislocations, station timing errors and unaccounted-for diffraction effects (Celli, Lebedev, Schaeffer, Ravenna, & Gaina, 2020; Lebedev & Van Der Hilst, 2008; Legendre et al., 2012).

3. Results

3.1. Model Description

The tomographic model provides new information on the distribution of low velocities beneath the rift system, as well as the deep structure of the adjacent Arabian Platform and Zagros subduction zone.

Our tomography reveals a star-shaped, low-velocity feature in the asthenosphere centered at Afar and composed of three branches beneath East Africa, the Gulf of Aden, and the Red Sea-western Arabia, the latter extending to Levant at the northwestern extremity of the Arabian Plate (Figure 4, 110-km depth slice). Low-velocity anomalies within the branches are all laterally continuous and exceed −6% in the shallow asthenosphere in most places. The recent LAB depth model of Fullea et al. (2021) confirms that this star-shaped low-velocity body coincides with areas of relatively thin lithosphere (Figure S1 in Supporting Information S1).

Below the EARS, the low-velocity anomaly spans from Afar to Tanzania and is exceptionally deep. It resembles a curtain of hot material extending down to over 400 km depth (Figure 4, cross-section A-B). In western Arabia, a low-velocity channel underlies the eastern margin of the Red Sea and extends down to ∼250 km depth (Figure 4, cross-section B-C). This elongated anomaly is stronger in amplitude ($dV_S \approx -8\%$ at 110 km depth) below the central-western volcanic sites ("harrats" 10–16, Figure 2b, 20–26°N) and weaker (−4%) to the north ("harrats" 8–9, Figure 2b, 26°–28°N) and, intriguingly, below the Red Sea (−2% to 4%). In the Levant region, the anomaly amplitude increases to −6%, and it bifurcates westwards to Anatolia and eastwards to the Caucasus. Beneath the Gulf of Aden, the shortest of the branches, a pronounced low-velocity anomaly (−6% at 110 km depth) extends

10.1029/2022GC010610

down to ~200 km depth. The extremely low velocities below all three branches suggest extensive partial melting in the uppermost mantle (e.g., Bastow et al., 2005; Kendall et al., 2005; Rooney et al., 2005). The global thermochemical model of the upper mantle WINTERC-G (Fullea et al., 2021) confirms estimates of 1%–2% melt beneath the area, and regional studies report melt fractions over 2% in Afar and western Arabia (e.g., A. H. Ahmed et al., 2016; George & Rogers, 2002).

Two low-velocity columns are imaged at the extremities of the "curtain" seismic anomaly below East Africa, one below Kenya-northern Tanzania and the other beneath Afar (Figure 4, cross-section A-B). They are connected to the "curtain" in the uppermost mantle and extend vertically through the mantle transition zone (MTZ; 410–660 km depth). Similarly to what proposed by previous studies (e.g., Chang et al., 2020; Nelson et al., 2012; Vicente de Gouveia et al., 2018), we interpret these features as the seismic expression of the Kenya Plume (KP) and the Afar Plume (AP), respectively.

Our tomography also shows a pronounced low-velocity anomaly in the MTZ beneath Iraq, connected to the Levant asthenospheric low-velocity corridor, adjacent to a strong high-velocity anomaly below the north-east Arabia likely correlated with thicker lithosphere (Figure 4, cross-section D-E). The anomaly in the MTZ indicates a hot mantle upwelling, which we name the Levant Plume (LP). Impinging onto the thick lithosphere of the Arabian Platform (see Figure S1 in Supporting Information S1), it appears to deflect westward, into the thin-lithosphere channel, and is likely to sustain most of the Levant volcanism. The lower amplitude of the low-velocity anomaly at 250–350 km depth is due, in part, to the lateral averaging of the tomography, which reduces the amplitudes in the model of both the lithospheric high-velocity anomaly beneath the Arabian Platform and the low-velocity anomaly of the hot material flowing along this lithospheric block's boundary.

3.2. Model Resolution

A series of resolution tests were performed to assess the accuracy of our model. We built a synthetic model with S-wave spike velocity anomalies (200 ms^{-1} amplitude) at 110, 200, 330, and 585 km depth nodes below different locations in the model. The two spikes shown Figures S2 and S3 in Supporting Information S1 are in different parts of the region and are widely spaced (one in the north, within the Levant region, and the other in the south of the Arabian Plate), which prevents interference of their output point-spread patterns (Rawlinson & Spakman, 2016). The output synthetic models recover well the locations of the input spikes at 110 and 200-km depth along both the vertical and horizontal axes (Figure S2 in Supporting Information S1). As expected, the deeper spikes (at 330- and 585-km depth) show greater spatial spreading of the velocity anomalies, but the maximum recovered amplitudes are positioned at the correct locations (Figure S3 in Supporting Information S1). Figure 5 and Figures S4, S5 in Supporting Information S1 show more complex resolution tests, where the seismic velocity structure below the EARS, western Arabia and Levant region had been removed partially (starting from 150 km depth in Figure 5 and above the MTZ in Figure S4 in Supporting Information S1) and completely (from 0 to 660 km depth in Figure S5 in Supporting Information S1) respectively. The tests confirm that if the low-velocity features, in particular the EARS "curtain" and the Levant anomalies, were not present in the Earth, then they would not appear in the model as a result of smearing due to insufficient data sampling. Thus, these anomalies are unlikely to be artifacts and our model resolves them accurately.

4. Discussion

4.1. Star-Shaped Plume Head Beneath the East African-Arabian Lithosphere

Evidence for elevated mantle temperatures beneath East Africa-Arabia has come from different lines of evidence. Mantle xenoliths derived from alkaline rocks in Saudi Arabia indicate abnormally high temperatures >1200°C at the top of the uppermost mantle beneath the Arabian shield (A. H. Ahmed et al., 2016; Mcguire & Bohannon, 1989). Geochemical analyses on EARS lavas found thermal anomalies of up to 170°C above the ambient upper mantle (Rooney et al., 2012). These values fall within the thermal excess range of 100–200°C estimated by converting seismic velocity to temperature through a thermodynamic approach (Civiero et al., 2015, 2016), numerical modeling of lithospheric extension and mantle melting (Armitage et al., 2015), petrogenic modeling (Ferguson et al., 2013) and receiver function analyses (Rychert et al., 2012). These temperature estimates are close to the low end of the global temperature range of LIPs (Rooney et al., 2012), despite the strong low-velocity anomalies imaged in the mantle. Deep partial melting is likely to be required to account for the low seismic

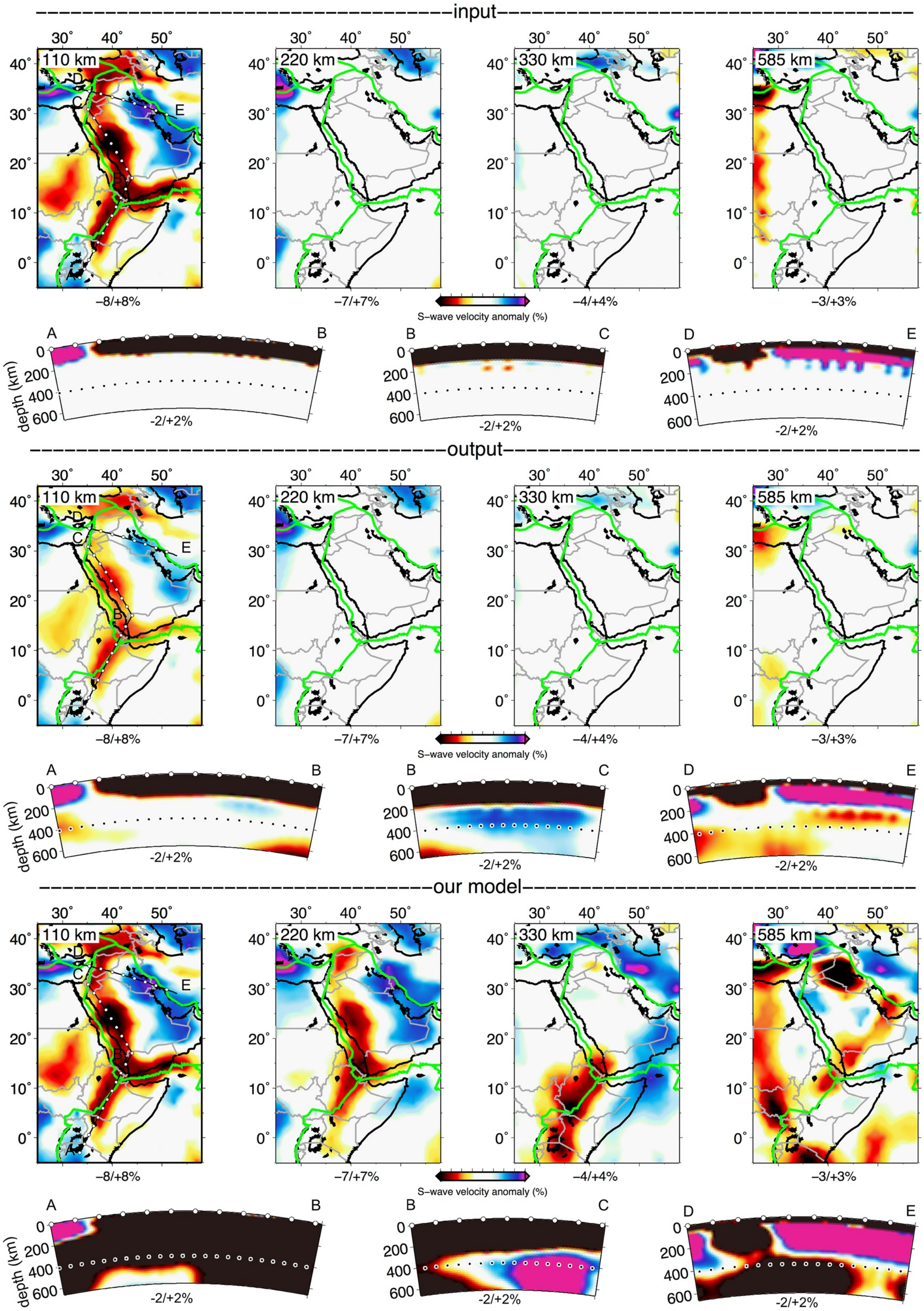
input
110 km
220 km
330 km
585 km
-8/+8%
-7/+7%
-4/+4%
-3/+3%
S-wave velocity anomaly (%)
A
B
C
D
E
depth (km)
-2/+2%
output
our model

Figure 5.

velocities. Plate stretching during rift development may have produced a large amount of decompression melt in the asthenosphere that can explain the low seismic velocities observed in the upper mantle beneath the region (e.g., Bastow et al., 2010). Rooney (2010, 2020a, 2020b) showed that melt sources beneath East Africa lie both in the lithosphere and convecting upper mantle and suggested that depleted mantle and lithospheric material may have mixed together with the AP melts.

The relatively high temperatures and melt in the asthenosphere, the pronounced uplift of the surface, and the temporal (pulsed) continuity of the volcanism since ∼45 Ma indicate that a single plume head may be ponding beneath the thin-lithosphere corridors. Ponding and channeling of hot plume material in thin-lithosphere areas, as well as plume viscous fingering in the asthenosphere, have been proposed previously (e.g., Ebinger & Sleep, 1998; Lees et al., 2020; Schoonman et al., 2017; Steinberger et al., 2019). However, direct observational evidence on the morphology and evolution of the volumes of hot rock, especially in the case of ancient LIPs, has been scarce or missing. Our detailed new images of the hot-rock volume beneath the East Africa-Arabia region, combined with the evidence from volcanism, suggests that this volume can, indeed, be seen as the plume head itself, resulting from three separate upwelling stems. The plume material would first have to occupy pre-existing areas with relatively thin lithosphere, beneath what is now the EARS and western Arabia, and then new ones were created by lithospheric stretching and rifting and by the thermo-chemical erosion of the lithosphere by the plume. This large body of hot, partially molten rock, occupying a system of interconnected thin-lithosphere channels, would have shaped as a three-pointed star with time and sustained all the broadly distributed, protracted, evolving LIP volcanism.

Lateral asthenospheric flow within the East Africa-Arabia plume head is evidenced by seismic anisotropy. Overall, shear-wave splitting measurements show the alignment of fast-propagation directions within the three branches parallel to the branch orientations (e.g., Bagley & Nyblade, 2013; Gao et al., 2010; Kendall et al., 2005, 2006; Qaysi et al., 2018). This is consistent with north-south flow of hot plume material within the western-Arabia branch and within the EARS 'curtain" anomaly and with eastward flow beneath the Gulf of Aden (Figure 4, Figure S6 in Supporting Information S1). Besides, a more recent study of mantle anisotropy (Andriampenomanana et al., 2021) found NNE-NE fast polarization directions further south, in northeastern Uganda and in southeastern Tanzania, which were attributed to an overall northerly orientation of the sublithospheric mantle flow across East Africa. We do not exclude, however, that a component of melt-induced anisotropy may play a role, contributing to SKS splitting together with the asthenospheric flow mechanism, in some locations, including the transitional northern Ethiopian Rift, as suggested by Kendall et al. (2006, 2005).

4.2. Three Deep Mantle Upwellings: Afar Plume, Kenya Plume, and Levant Plume

The low-velocity anomalies that we map beneath the East Africa-Arabia region are confirmed by other regional tomographic models, computed with other data and methods (e.g., Bastow et al., 2008; Chang & Van der Lee, 2011; Civiero et al., 2019; Koulakov et al., 2016; Montagner et al., 2007; Sicilia et al., 2008; Yao et al., 2017). Some studies image connected low-velocity anomalies in the upper mantle beneath the EARS and western Arabia (Chang & Van der Lee, 2011; Debayle et al., 2001; Montagner et al., 2007; Sicilia et al., 2008). Other seismic models show separated and localized low-velocity bodies below Ethiopia and Kenya (Bastow et al., 2008; Montelli et al., 2006; Park & Nyblade, 2006). The overall similarity with the other models provides further evidence for the presence of partially molten rock beneath the region, which rather than spreading as a circle and disappearing, has morphed into a complex shape by the LAB (Figure 1). Our model offers an improvement compared to previous studies as it clearly shows that this body extends continuously along the three thin-lithosphere corridors, with anomaly amplitude lower than −6% everywhere within them, which requires high temperature and partial melting (e.g., Armitage et al., 2015; Civiero et al., 2016; Fullea et al., 2021; Rooney et al., 2012).

The sprawling plume head continues to be fed by hot upwellings from the deep mantle. The (sub-)vertical low-velocity anomalies interpreted as the tails of the three mantle plumes have been imaged in generally similar

Figure 5. Structural resolution test 1. The seismic structure below the East Africa-Arabia region are removed in the input (top panels) at depths ≥150 km. The output model (middle panels) shows that the curtain-like anomaly does not appear at depths greater than 150 km, thus confirming that it is a real feature in our model and that the Kenya Plume and Afar Plume extend through the transition zone. Although an amount of spurious structure is mapped in the transition zone below the Levant region, the amplitude of the anomaly is much weaker than that imaged in our model (bottom panels) and does not impact the interpretation of the Levant Plume. The orientations of the cross-sections are plotted in the 110-km depth slice and are the same as those in Figure 4. Major plate boundaries are plotted as green lines. White points indicate the distance every 2°. The dotted line in the cross-sections indicates the 410-km depth discontinuity.

positions in the S-wave tomography model of Chang and Van der Lee (2011), using a different data set and methodology. Having resolution also in the lower mantle, their model shows that the anomalies extend deeper than the MTZ down to at least 1,400-km depth. Our upper-mantle results also show broad agreement with the continental-scale ambient-noise tomography images of Emry et al. (2019), which provide evidence of two distinct low-velocity features below Afar and Kenya in the MTZ. By contrast, Hansen et al. (2012) found in their P-wave tomography a single upper-mantle low-velocity anomaly beneath East Africa-Arabia and interpreted it as the shallower continuation of the African Superplume. The recent P-wave model of Boyce et al. (2021) suggests, instead, that this single anomaly may split in two below the MTZ. Moreover, although not discussed in their work, another strong low-velocity feature is imaged below the Levant region, exactly where we locate the tilted LP. This is also consistent with the P-wave model of Koulakov et al. (2016), which images a tilted low-velocity anomaly below the Arabian Plate, interpreted as a hot mantle upwelling deflected westward by the Arabian Platform after impinging onto its thick lithosphere.

The elevated temperatures in the MTZ indicated by the low velocities where the three plumes (AP, KP, and LP) rise through it are confirmed by independent evidence from several receiver-function studies. Differential arrival times of the P-to-S conversions at the 660- and 410-km discontinuities indicate anomalously thin—and, thus, anomalously hot (e.g., Lebedev et al., 2003)—MTZ below Iraq, Afar, and Kenya (Boyce & Cottaar, 2021; Kaviani et al., 2018; Mulibo & Nyblade, 2013; Sun et al., 2017; Thompson et al., 2015) (Figure 6).

Whole-mantle, body-wave tomography yields further complementary evidence on the deep plume structure. The surface-wave and regional body-wave waveforms that constrain our model offer the best available sampling of the lithosphere and asthenosphere, with resolution down to the MTZ. The teleseismic body-wave tomography, by contrast, has the best resolution in regions with dense coverage with crossing teleseismic rays, normally in the lower mantle and the MTZ (and in the upper mantle beneath regions with a lot of seismic stations or sources). Body-wave tomography models confirm the plume anomalies we identify in the MTZ (Figure 7, Figure S7 in Supporting Information S1). In particular, the high-resolution UU-P07 model (Amaru, 2007) shows similar low-velocity anomalies extending through the MTZ beneath Kenya, Afar and Levant regions, confirming the occurrence of the three plumes (Figure 7). It can also complement our results by providing information on the continuity of the anomalies into the lower mantle. The anomaly beneath Kenya extends down to the core-mantle boundary, whereas the structure beneath Afar and Levant is more complex, with prominent high-velocity anomalies disrupting the continuity of the low-velocity columns (Figure 7, Figures S8 and S9 in Supporting Information S1).

Most global tomography models capture a high-velocity body that truncates the Levant low-velocity feature in the lower mantle (in the ∼1,200 to 1,800 km depth range) and connects with the high-velocity anomalies at the same depths below Afar (Figure 7, cross-section D-E and Figure S8 in Supporting Information S1). According to a recent catalog of subduction zones of van der Meer et al. (2018), the high-velocity anomaly is probably the Arabian slab, subducted northeastward along the Eurasian margin during the Late Cretaceous. This body has been identified also in the recent work of Chang et al. (2020) as the subducted Tethyan slab, which interacted with the AP and detached it from the core-mantle boundary. Our "vote map" images suggest that the AP and LP may originate from the same source region at the core-mantle boundary below Arabia-offshore Somalia. This would be in agreement with the hypothesis proposed by Koulakov et al. (2016), of a mantle plume beneath the Arabia Peninsula tilting toward west and feeding the surface volcanism. Subducting lithosphere from an ancient subduction system may be disrupting the upwelling in the lower mantle and splitting it into narrower plumes beneath Afar and Levant. Alternatively, the two plumes may be entirely separate, as proposed by Boyce et al. (2021), and both perturbed and deflected by the sinking slab material (Chang et al., 2020) (Figure S10 in Supporting Information S1).

The "curtain" seismic anomaly below East Africa—a narrow, dyke-like feature extending from the surface into the MTZ—is a exceptional phenomenon, observed nowhere else on Earth, according to global tomography (e.g., French & Romanowicz, 2014; Schaeffer & Lebedev, 2013). Its location between the AP and KPs, located only 1,000 km from each other, is likely to be responsible for its formation, with the flow of hot material in the upper mantle between the two upwellings the probable mechanism. Our model shows that the EARS "curtain" anomaly is continuous and nearly uniform at the scales of a few 100 km. Superimposed on this large-scale pattern, it may also comprise smaller-scale heterogeneity, detected by regional tomographic studies (Civiero et al., 2016, 2019).

10.1029/2022GC010610

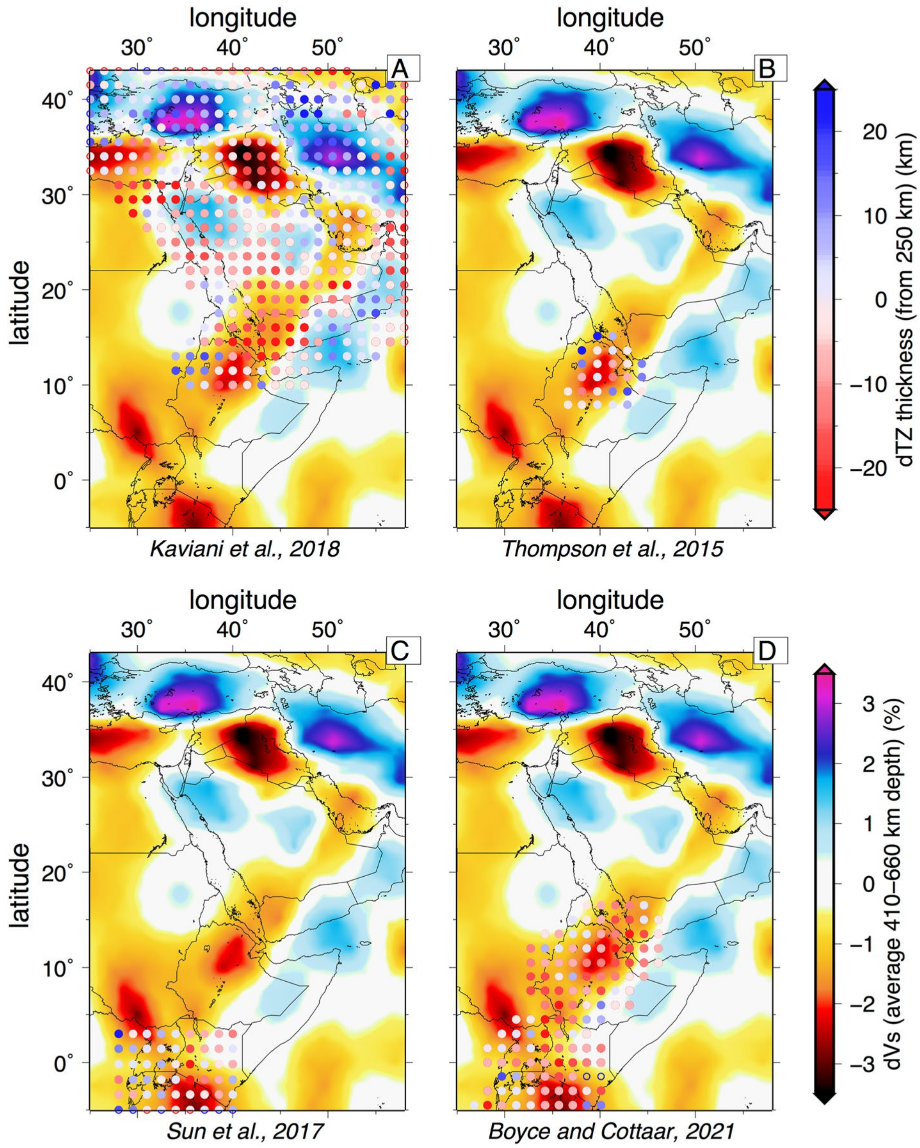

Figure 6. Transition zone thickness from P-wave receiver functions and the average S-wave velocity anomaly within the transition zone. The points, spaced at 1.5°, show the transition zone thickness anomaly from Kaviani et al. (2018) (a), Thompson et al. (2015) (b), Sun et al. (2017) (c), and Boyce and Cottaar (2021) (d). The nearneighbor interpolation method available in GMT is used. Negative values indicate thinning of the transition zone; positive values indicate thickening of the transition zone relative to the reference value of 250 km. The maps also show the average shear-wave speed (dV_S) anomaly in the 410–660 km depth range, according to our tomography. Note the consistency between the location of the subduction zones in the north and the thickening of the transition zone. There is also a strong correlation at the location of the Levant Plume, Afar Plume, and Kenya Plume stems between the thinning of the transition zone and the low-velocity anomalies, with both independent lines of evidence indicating anomalously high temperatures.

4.3. Evolution of the East Africa-Arabia System

Basaltic rock ages show that the EARS volcanism first started in southern Ethiopia at ~45 Ma with a low eruption rate (~0.003 km^3 yr^{-1}) (Davidson & Rex, 1980; Ebinger et al., 1993; George et al., 1998; Rooney, 2017) (Figure 2). At that time, plate-tectonic reconstructions locate the KP below northern Ethiopia (see Figure 8, Figure S11, and Text S2 in Supporting Information S1). Assuming stationary plumes beneath moving lithospheric plates, this suggests that the KP has thermo-mechanically eroded the lithosphere and caused the early flood basalts in southern Ethiopia, once the lithospheric thinning was sufficient to sustain substantial decompression melting. After the impingement, the KP formed a NNE-SSW-oriented line of volcanic edifices, termi-

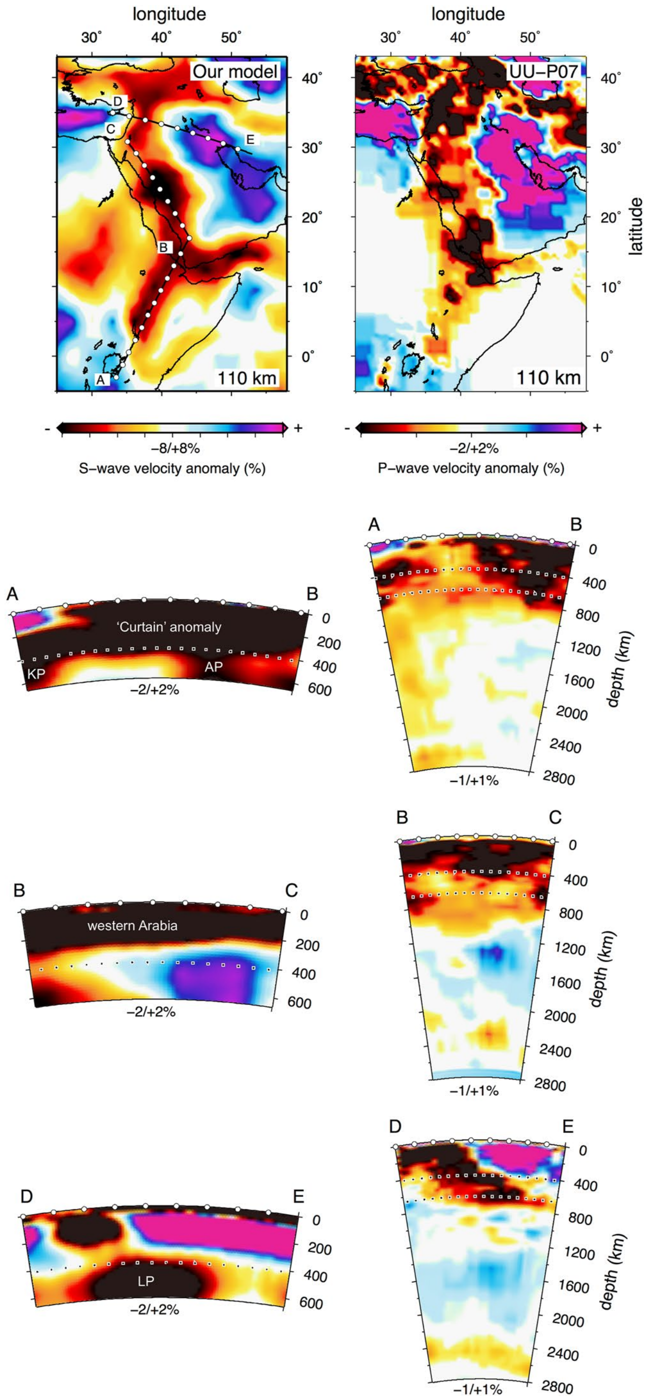

Figure 7. Comparison of our tomographic model with the global P-wave model UU-P07. The map views (top panels) are plotted at 110 km depth. The orientations of the cross-sections are plotted in the 110-km depth map view of our model and are the same as in Figure 4. The dotted lines indicate the 410- and 660-km depth discontinuities. White points indicate the distance every 2°.

nating around Lake Victoria where the plume is currently located. To the north, the AP impacted the thick Arabian Platform lithosphere at ~30 Ma and triggered abundant volcanism in the northern Ethiopia-Yemen area (the Red Sea was not formed yet), where the lithosphere was thinner. The great volume of these flood basalts is reflected in a peak in volcanism at this time (~0.024 $km^3\ yr^{-1}$ eruption rate) (Ebinger et al., 1993; George et al., 1998; Rooney, 2017), followed by another, lower peak (~0.09 $km^3\ yr^{-1}$) in the Late Neogene, associated with the current activity of the AP (George et al., 1998) (Figure 2b). At 20–30 Ma, the LP impacted the base of the thick Arabian Platform lithosphere (Stern & Johnson, 2010). The plume material ascended westward into a thinner-lithosphere area and gave rise to the volcanism in the Levant region, eventually merging with the plume material beneath western Arabia (Figure 9). The more localized volcanic events occurring after ~20 Ma are likely associated with lithospheric extension and focused on the developing rift (Rooney, 2017). However, it is now evident from our new tomographic observations that the plumes continue to influence volcanism in extending areas throughout the region.

The rate of the southward propagation of the East-African volcanism in the Africa reference frame (Figure 2c) does not exceed the rate of Africa's northward absolute plate motion (Figure 8). This indicates that the KP material did not flow south beneath Africa, probably due to the lack of a suitable thin-lithosphere channel. The passage over the KP, however, may have thinned the African lithosphere, facilitating the flow of the plume material northward. A contribution of mantle material flowing northerly and trigger for flood-basalt volcanism may be attributed to an another plume located between the KP and AP, as evidenced by the paleo-reconstruction model of Vicente de Gouveia et al. (2018).

The active, star-shaped plume head ponded below the East African-Arabian lithosphere is a unique feature on the Earth at present. Its structure and evolution, however, give us an insight into the likely mechanism of emplacement of many continental LIPs. The volcanism in the Central Atlantic Magmatic Province and the North Atlantic Igneous Province, for example, is protracted in time and dispersed over areas thousands of kilometers across and it has been debated whether they could be considered single magmatic provinces at all (Beccaluva et al., 2020; Steinberger et al., 2019). Similarly to what we are observing today in East Africa-Arabia, variations in the continental lithosphere thickness—pre-existing and unrelated to rifting and evolving due to rifting and plume-lithosphere interaction—must have morphed plume heads into star-like shapes at the base of the lithosphere and caused the enigmatic broad and uneven distributions of volcanism in these and other LIPs (Ebinger & Sleep, 1998; Peace et al., 2020; Steinberger et al., 2019).

If we consider the plume head, broadly, as the large volume of plume material ponding and spreading beneath the lithosphere and supplied via the thin plume stem (Morgan, 1971; Sleep, 1997; White & McKenzie, 1989), then a star shape of this volume can explain, for example, the widely distributed volcanism that occurred in the North Atlantic Igneous Province just before the opening of the northeast Atlantic Ocean. In this case, one of the thin-lithosphere corridors cut east-west across central Greenland, likely created by the passage of Greenland over the Iceland Plume (Lebedev et al., 2018). The corridor then provided a conduit for the flow of the Iceland Plume material that is thought to have produced the simultaneous volcanism at the western and eastern coasts of Greenland (Steinberger et al., 2019). Other thin-lithosphere areas extending toward Ireland, Britain and Norway, may have channeled the plume material eastwards and given rise to the volcanism in these regions (Lebedev et al., 2021; Rickers et al., 2013; White & Lovell, 1997). Shortly

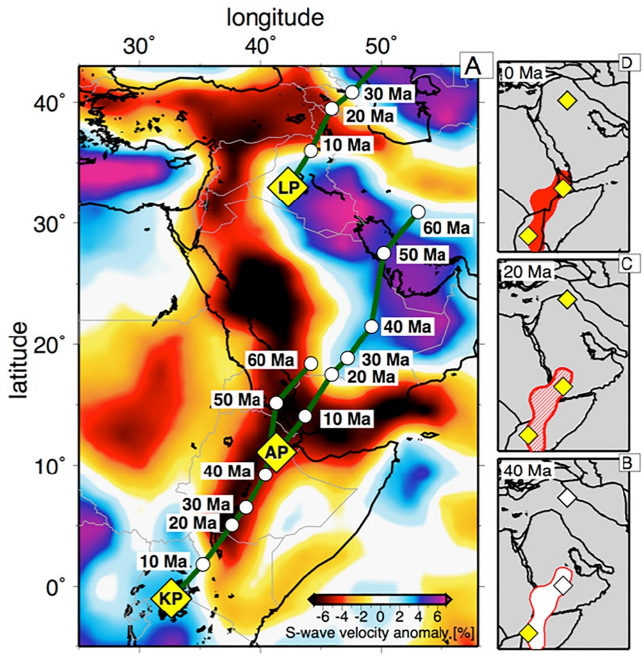

Figure 8. Hotspot tracks and plate-tectonic reconstructions. (a) Tracks of the Afar, Kenya, and Levant Plumes (AP, KP, and LP; yellow diamonds), according to the plate-tectonic reconstruction of Torsvik et al. (2019). The seismic tomography model plotted in the map view is at 110 km depth. (b–d) Plate-tectonic reconstructions at 40 Ma (b) and 20 Ma (c) and the present-day map (d). The red structure highlighted is the "curtain" low-velocity anomaly beneath EARS, enclosed by a $dVs = -2.5\%$ contour. At 40 Ma (b), the curtain has not formed yet (white), the KP has arrived at the base of the lithosphere (yellow diamond), and AP and LP are still rising in the mantle (white diamonds). At 20 Ma (c), the material from the three plumes—KP, AP and LP—is spreading below the lithosphere and feeding volcanism at the surface (yellow diamonds), with the curtain developing. At present (d), the curtain anomaly between KP and AP has formed, and the three plumes are all active.

after the opening of the northeast Atlantic Ocean, the plume material was captured in the thin-lithosphere valleys beneath the Mid-Atlantic Ridge (Celli et al., 2021; Sleep, 1997; Steinberger et al., 2019). In the Central Atlantic Magmatic Province, voluminous flood basalts cover a large area in South America that is underlain by a corridor of relatively thin lithosphere, situated between thick cratonic blocks (Boscaini et al., 2022; Celli, Lebedev, Schaeffer, Ravenna, & Gaina, 2020; Chagas De Melo et al., 2022), which indicates that a large volume of plume material was channeled into it. These examples illustrate that the thin-lithosphere channels can be created not only by rifts, such as those radiating from the Afar triple junctions, but also by other processes, such as the passage of a lithospheric plate above the plume, or simply be pre-existing areas of thinner lithosphere. Numerical modeling studies corroborate the idea that the passage of a plate over a plume can erode lithosphere and create thin-lithosphere channels (e.g., Burov & Gerya, 2014; Heyn & Conrad, 2022; Koptev et al., 2017, 2018; Sobolev et al., 2011).

5. Conclusions

The East Africa-Arabia region is the one place on Earth where we can witness plume-lithosphere interaction in the context of a LIP emplacement. Like many ancient LIPs, it features volcanism scattered over a very broad area and protracted in time. Unlike with ancient LIPs, here we can observe the large body of hot, partially molten rock that extends beneath all the volcanic areas and, in all probability, gives rise to most of the sustained volcanism. We interpret our tomography as a snapshot of an extant, integral plume head, developing over the last ~45 Ma and contained within a system of thin-lithosphere corridors. The plume-lithosphere interaction, suggested by our results, is characterized by a complex feedback between the lithospheric thickness variations, ponding and channeling of hot material in thinner-lithosphere areas, and the thinning of the lithosphere due to rifting and erosion by the hot plume material.

10.1029/2022GC010610

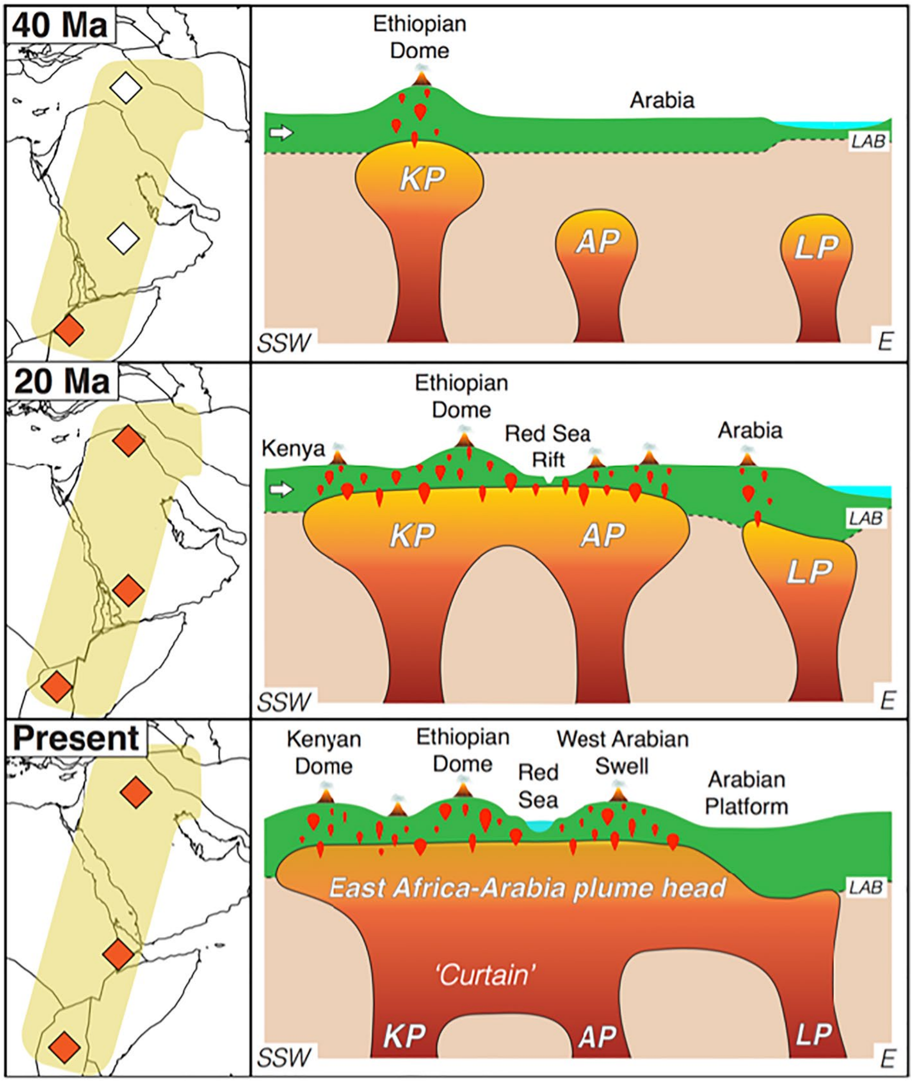

Figure 9. Evolution of the East Africa-Arabia plume head. The light-brown band on the maps indicates the location of the schematic cross-section. 40 Ma: the Kenya Plume impacted the lithosphere and generated volcanism below Ethiopia, with the Afar and Levant Plumes still rising in the mantle. 20 Ma: the plume material merged between the Kenya and Afar Plume stems, with volcanism observed throughout, and the Levant Plume reached the lithosphere in the Mesopotamia region. At present, the three plumes are feeding an integral East Africa-Arabia plume head, with dispersed volcanism and surface uplift above it.

Conflict of Interest

The authors declare no conflicts of interest relevant to this study.

Data Availability Statement

Seismic data from network codes marked in Figure 3 were freely available from several data centers including: the IRIS Data Management Center (https://ds.iris.edu/ds/nodes/dmc/); the GEOFON Data Centre of the GFZ (https://geofon.gfz-potsdam.de/waveform/archive); the RESIF seismic data portal (https://seismology.resif.fr/); Observatories and Research Facilities for European Seismology (http://orfeus-eu.org/webdc3/); the National Observatory of Athens (http://bbnet.gein.noa.gr); the Turkish Earthquake Research Institute KOERI (http://eida-service.koeri.boun.edu.tr); and the Italian Istituto Nazionale di Geofisica e Vulcanologia INGV (http://webservices.ingv.it). Table S2 in Supporting Information S1 provides details on the network and station codes

Acknowledgments

We thank two anonymous reviewers and the Editor, Maureen Long, whose comments and suggestions have helped us to improve the manuscript. We are grateful to the operators of the seismic networks in Africa, Arabia, Turkey and elsewhere for collecting the seismic data, including data in the following experiments: the Ethiopia Afar Geoscientific Lithospheric Experiment, EAGLE (Bastow et al., 2005; Mackenzie et al., 2005; Maguire et al., 2003; Stuart et al., 2002), the Ethiopia/Kenya Broadband Seismic Experiment, EKBSE (Bastow et al., 2008; Benoit et al., 2006; Hammond et al., 2013; Nyblade & Langston, 2002), the AfricaArray (Nyblade et al., 2008, 2011), the Afar Consortium project (Belachew et al., 2011; Hammond et al., 2011), the Afar Urgency Array (Ebinger et al., 2008; Keir et al., 2009), the Réseau Large Bande Mobile, RLBM (Sebai et al., 2006), the Dhofar Seismic Experiment (Basuyau et al., 2010), the Young Conjugate Margins Laboratory, YOCMAL (A. Ahmed et al., 2013; Leroy et al., 2007), the Tanzania Broadband Seismic Experiment, TBSN (Brazier et al., 2000; Nyblade et al., 1996), the Saudi Arabian Broadband Experiment, SABA (Sandvol et al., 1998, 2001), the Hellenic Unified Seismological Network, HUSN (D'Alessandro et al., 2011; Evangelidis & Melis, 2012), the Aristotle University of Thessaloniki Seismological Network, AUTHnet (Pitilakis et al., 2016), the Eastern Turkey Seismic Experiment (Sandvol et al., 2003), the Turkish National Seismic Network (Al-Lazki et al., 2003), the Kaapvaal Project (P. Silver et al., 2016), the Seismic Imaging of the Mantle in the Aegean-Anatolian Domain SIMBAAD Experiment (Paul et al., 2008); the Jordan Seismic Network (Rodgers et al., 2003); the EGELADOS seismic monitoring project (Friederich & Meier, 2008), the National Seismic Network of Georgia (Tumanova et al., 2016); the DESERT project (Mechie et al., 2005; Mohsen et al., 2006), the Dead Sea Integrated Research project DESIRE (Mechie et al., 2009), and the Cyclades seismic network CYCNET and Lybian Sea Network LIBNET (Bohnhoff et al., 2006). We thank Angelo De Min for the insightful discussions. The figures were generated with the Generic Mapping Tools (Wessel et al., 2013), and Illustrator (https://adobe.com/products/illustrator). This work was supported by the Science Foundation Ireland (SFI) Grants 13/CDA/2192 and 16/IA/4598, the latter co-funded by the Geological Survey of Ireland and the Marine Institute. This work has been completed in the framework of the project 3D Earth funded by the European Space Agency (ESA) as a Support to Science Element (STSE). C.C. acknowledges the grant CEX2019-000928-S funded by AEI 10.13039/501100011033.

downloaded from each data center. We thank all the network operators who contributed data to these data centers. The tomographic model is available to download at https://nlscelli.wixsite.com/ncseismology/af2019. It is also deposited to the online IRIS EMC-Earth Models repository (https://doi.org/10.17611/dp/emc.2022.af2019.1).

References

Ahmed, A., Tiberi, C., Leroy, S., Stuart, G. W., Keir, D., Sholan, J., et al. (2013). Crustal structure of the rifted volcanic margins and uplifted plateau ofwestern Yemen from receiver function analysis. *Geophysical Journal International*, *193*(3), 1673–1690. https://doi.org/10.1093/gji/ggt072

Ahmed, A. H., Moghazi, A. K. M., Moufti, M. R., Dawood, Y. H., & Ali, K. A. (2016). Nature of the lithospheric mantle beneath the Arabian shield and Genesis of Al-spinel micropods: Evidence from the mantle xenoliths of Harrat Kishb, Western Saudi Arabia. *Lithos*, *240–243*, 119–139. https://doi.org/10.1016/j.lithos.2015.11.016

Al Kwatli, M. A., Gillot, P. Y., Zeyen, H., Hildenbrand, A., & Al Gharib, I. (2012). Volcano-tectonic evolution of the northern part of the Arabian plate in the light of new K-Ar ages and remote sensing: Harrat Ash Shaam volcanic province (Syria). *Tectonophysics*, *580*, 192–207. https://doi.org/10.1016/j.tecto.2012.09.017

Al-Lazki, A. I., Seber, D., Sandvol, E., Turkelli, N., Mohamad, R., & Barazangi, M. (2003). Tomographic Pn velocity and anisotropy structure beneath the Anatolian plateau (eastern Turkey) and the surrounding regions. *Geophysical Research Letters*, *30*(24), 4–7. https://doi.org/10.1029/2003GL017391

Amaru, M. L. (2007). Global travel time tomography with 3-D reference models. *Geologica Ultraiectina*, *274*, 174.

Andriampenomanana, F., Nyblade, A., Durrheim, R., Tugume, F., & Nyago, J. (2021). Shear wave splitting measurements in northeastern Uganda and southeastern Tanzania: Corroborating evidence for sublithospheric mantle flow beneath East Africa. *Geophysical Journal International*, *226*(3), 1696–1704. https://doi.org/10.1093/gji/ggab167

Armitage, J. J., Ferguson, D. J., Goes, S., Hammond, J. O. S., Calais, E., Rychert, C. A., & Harmon, N. (2015). Upper mantle temperature and the onset of extension and break-up in Afar, Africa. *Earth and Planetary Science Letters*, *418*, 78–90. https://doi.org/10.1016/j.epsl.2015.02.039

Bagley, B., & Nyblade, A. A. (2013). Seismic anisotropy in eastern Africa, mantle flow, and the African superplume. *Geophysical Research Letters*, *40*(8), 1500–1505. https://doi.org/10.1002/grl.50315

Baker, J. A., Thirlwall, M. F., & Menzies, M. A. (1996). Sr-Nd-Pb isotopic and trace element evidence for crustal contamination of plume-derived flood basalts: Oligocene flood volcanism in Western Yemen. *Geochimica et Cosmochimica Acta*, *60*(14), 2559–2581. https://doi.org/10.1016/0016-7037(96)00105-6

Ballmer, M. D., van Keken, P. E., & Ito, G. (2015). Hotspots, large igneous provinces, and melting anomalies. In *Treatise on Geophysics* (2nd ed., Vol. 7). Elsevier B.V. https://doi.org/10.1016/B978-0-444-53802-4.00133-0

Bassin, C., Laske, G., & Masters, G. (2000). The current limits of resolution for surface wave tomography in North America. *EOS*, *81*, F897.

Bastow, I. D., & Keir, D. (2011). The protracted development of the continent-ocean transition in Afar. *Nature Geoscience*, *4*(4), 248–250. https://doi.org/10.1038/ngeo1095

Bastow, I. D., Nyblade, A. A., Stuart, G. W., Rooney, T. O., & Benoit, M. H. (2008). Upper mantle seismic structure beneath the Ethiopian hot spot: Rifting at the edge of the African low-velocity anomaly. *Geochemistry, Geophysics, Geosystems*, *9*(12), Q12022. https://doi.org/10.1029/2008gc002107

Bastow, I. D., Pilidou, S., Kendall, J. M., & Stuart, G. W. (2010). Melt-induced seismic anisotropy and magma assisted rifting in Ethiopia: Evidence from surface waves. *Geochemistry, Geophysics, Geosystems*, *11*(6), 1–19. https://doi.org/10.1029/2010GC003036

Bastow, I. D., Stuart, G. W., Kendall, J. M., & Ebinger, C. J. (2005). Upper-mantle seismic structure in a region of incipient continental breakup: Northern Ethiopian Rift. *Geophysical Journal International*, *162*(2), 479–493. https://doi.org/10.1111/j.1365-246X.2005.02666.x

Basuyau, C., Tiberi, C., Leroy, S., Stuart, G., Al-Lazki, A., Al-Toubi, K., & Ebinger, C. (2010). Evidence of partial melting beneath a continental margin: Case of Dhofar, in the Northeast Gulf of Aden (Sultanate of Oman). *Geophysical Journal International*, *180*(2), 520–534. https://doi.org/10.1111/j.1365-246X.2009.04438.x

Beccaluva, L., Bianchini, G., Natali, C., & Siena, F. (2020). Plume-related Paranà-Etendeka igneous province: An evolution from plateau to continental rifting and breakup. *Lithos*, *362–363*, 105484. https://doi.org/10.1016/j.lithos.2020.105484

Belachew, M., Ebinger, C., Coté, D., Keir, D., Rowland, J. V., Hammond, J. O. S., & Ayele, A. (2011). Comparison of dike intrusions in an incipient seafloor – Spreading segment in Afar, Ethiopia. Seismicity perspectives. *Journal of Geophysical Research: Solid Earth*, *116*(B6), 1–23. https://doi.org/10.1029/2010JB007908

Benoit, M. H., Nyblade, A. A., Owens, T. J., & Stuart, G. (2006). Mantle transition zone structure and upper mantle S velocity variations beneath Ethiopia: Evidence for a broad, deep-seated thermal anomaly. *Geochemistry, Geophysics, Geosystems*, *7*(11), Q11013. https://doi.org/10.1029/2006GC001398

Benoit, M. H., Nyblade, A. A., VanDear, J. C., & Gurrola, H. (2003). Upper mantle P wave velocity structure and transition zone thickness beneath the Arabian Shield. *Geophysical Research Letters*, *30*(10), 3–6. https://doi.org/10.1029/2002gl016436

Bercovici, D., & Mahoney, J. (1994). Double flood basalts and plume head separation at the 660-kilometer discontinuity author(s): David Bercovici and John Mahoney. *Science*, *266*(5189), 1367–1369. https://doi.org/10.1126/science.266.5189.1367

Bohannon, R. G., Naeser, C. W., Schmidt, D. L., & Zimmermann, R. A. (1989). The timing of uplift, volcanism, and rifting peripheral to the Red Sea: A case for passive rifting? *Journal of Geophysical Research*, *94*(B2), 1683–1701. https://doi.org/10.1029/jb094ib02p01683

Bohnhoff, M., Rische, M., Meier, T., Becker, D., Stavrakakis, G., & Harjes, H. P. (2006). Microseismic activity in the Hellenic Volcanic Arc, Greece, with emphasis on the seismotectonic setting of the Santorini-Amorgos zone. *Tectonophysics*, *423*(1–4), 17–33. https://doi.org/10.1016/j.tecto.2006.03.024

Boscaini, A., Marzoli, A., Bertrand, H., Chiaradia, M., Jourdan, F., Faccenda, M., et al. (2022). Cratonic keels controlled the emplacement of the Central Atlantic Magmatic Province (CAMP). *Earth and Planetary Science Letters*, *584*, 117480. https://doi.org/10.1016/j.epsl.2022.117480

Boyce, A., Bastow, I. D., Cottaar, S., Kounoudis, R., De Courbeville, J. G., Caunt, E., & Desai, S. (2021). AFRP20: New P-wavespeed model for the African mantle reveals two whole-mantle plumes below East Africa and neoproterozoic modification of the Tanzania craton. *Geochemistry, Geophysics, Geosystems*, *22*(3), e2020GC009302. https://doi.org/10.1029/2020gc009302

Boyce, A., & Cottaar, S. (2021). Insights into deep mantle thermochemical contributions to African magmatism from converted seismic phases. *Geochemistry, Geophysics, Geosystems*, *22*(3), 1–25. https://doi.org/10.1029/2020GC009478

Brazier, R. A., Nyblade, A. A., Langston, C. A., & Owens, T. J. (2000). Pn wave velocities beneath the Tanzania Craton and adjacent rifted mobile belts, East Africa. *Geophysical Research Letters*, *27*(16), 2365–2368. https://doi.org/10.1029/2000GL011586

Bryan, S. E., & Ernst, R. E. (2008). Revised definition of large igneous provinces (LIPs). *Earth-Science Reviews*, *86*(1–4), 175–202. https://doi.org/10.1016/j.earscirev.2007.08.008

Burov, E., & Gerya, T. (2014). Asymmetric three-dimensional topography over mantle plumes. *Nature*, *513*(7516), 85–89. https://doi.org/10.1038/nature13703

Burov, E., Guillou-Frottier, L., d'Acremont, E., Le Pourhiet, L., & Cloetingh, S. (2007). Plume head-lithosphere interactions near intra-continental plate boundaries. *Tectonophysics*, *434*(1–4), 15–38. https://doi.org/10.1016/j.tecto.2007.01.002

Camp, V. E. (1995). Mid-Miocene propagation of the Yellowstone mantle plume head beneath the Columbia River basalt source region. *Geology*, *23*(5), 435–438. https://doi.org/10.1130/0091-7613(1995)023<0435:MMPOTY>2.3.CO;2

Camp, V. E., & Roobol, M. J. (1992). Upwelling asthenosphere beneath Western Arabia and its regional implications. *Journal of Geophysical Research*, *97*(B11), 15255–15271. https://doi.org/10.1029/92jb00943

Campbell, I. H., & Griffiths, R. W. (1990). Implications of mantle plume structure for the evolution of flood basalts. *Earth and Planetary Science Letters*, *99*(1–2), 79–93. https://doi.org/10.1016/0012-821X(90)90072-6

Celli, N. L., Lebedev, S., Schaeffer, A., & Gaina, C. (2020). African cratonic lithosphere carved by mantle plumes. *Nature Communications*, *11*(1), 92. https://doi.org/10.1038/s41467-019-13871-2

Celli, N. L., Lebedev, S., Schaeffer, A. J., & Gaina, C. (2021). The tilted Iceland Plume and its effect on the North Atlantic evolution and magmatism. *Earth and Planetary Science Letters*, *569*, 117048. https://doi.org/10.1016/j.epsl.2021.117048

Celli, N. L., Lebedev, S., Schaeffer, A. J., Ravenna, M., & Gaina, C. (2020). The upper mantle beneath the South Atlantic Ocean, South America and Africa from waveform tomography with massive datasets. *Geophysical Journal International*, *221*(1), 178–204. https://doi.org/10.1093/gji/ggz574

Chagas De Melo, B., Lebedev, S., Celli, N., & Assumpção, M. (2022). Detailed structure of the South American cratons from seismic tomography. https://doi.org/10.22564/17cisbgf2021.098

Chang, S.-J., Ferreira, A. M. G., Ritsema, J., Heijst, H. J., & Woodhouse, J. H. (2015). Joint inversion for global isotropic and radially anisotropic mantle structure including crustal thickness perturbations. *Journal of Geophysical Research: Solid Earth*, *120*(6), 4278–4300. https://doi.org/10.1002/2014JB011824

Chang, S.-J., Kendall, E., Davaille, A., & Ferreira, A. M. G. (2020). The evolution of mantle plumes in East Africa. *Journal of Geophysical Research: Solid Earth*, *125*(12), e2020JB019929. https://doi.org/10.1029/2020JB019929

Chang, S.-J., Merino, M., Van Der Lee, S., Stein, S., & Stein, C. A. (2011). Mantle flow beneath Arabia offset from the opening Red Sea. *Geophysical Research Letters*, *38*(4), 1–5. https://doi.org/10.1029/2010GL045852

Chang, S.-J., & Van der Lee, S. (2011). Mantle plumes and associated flow beneath Arabia and East Africa. *Earth and Planetary Science Letters*, *302*(3–4), 448–454. https://doi.org/10.1016/j.epsl.2010.12.050

Chorowicz, J. (2005). The East African Rift System. *Journal of African Earth Sciences*, *43*(1–3), 379–410. https://doi.org/10.1016/j.jafrearsci.2005.07.019

Civiero, C., Armitage, J. J., Goes, S., & Hammond, J. O. S. (2019). The seismic signature of upper-mantle plumes: Application to the Northern East African rift. *Geochemistry, Geophysics, Geosystems*, *20*(12), 6106–6122. https://doi.org/10.1029/2019GC008636

Civiero, C., Goes, S., Hammond, J. O. S., Fishwick, S., Ahmed, A., Ayele, A., et al. (2016). Small-scale thermal upwellings under the northern East African Rift from S travel time tomography. *Journal of Geophysical Research: Solid Earth*, *2010*(10), 1–14. https://doi.org/10.1002/2016JB013070

Civiero, C., Hammond, J. O. S., Goes, S., Fishwick, S., Ahmed, A., Ayele, A., et al. (2015). Multiple mantle upwellings in the transition zone beneath the northern East-African Rift system from relative P-wave travel-time tomography. *Geochemistry, Geophysics, Geosystems*, *16*(9), 2949–2968. https://doi.org/10.1002/2015GC005948

Corti, G. (2009). Continental rift evolution: From rift initiation to incipient break-up in the Main Ethiopian Rift, East Africa. *Earth-Science Reviews*, *96*(1–2), 1–53. https://doi.org/10.1016/j.earscirev.2009.06.005

Courtillot, V., Davaille, A., Besse, J., & Stock, J. (2003). Three distinct types of hotspots in the Earth's mantle. *Earth and Planetary Science Letters*, *205*(3–4), 295–308. https://doi.org/10.1016/S0012-821X(02)01048-8

Cserepes, L., & Yuen, D. A. (2000). On the possibility of a second kind of mantle plume. *Earth and Planetary Science Letters*, *183*(1–2), 61–71. https://doi.org/10.1016/S0012-821X(00)00265-X

D'Alessandro, A., Papanastassiou, D., & Baskoutas, I. (2011). Hellenic unified seismological network: An evaluation of its performance through SNES method. *Geophysical Journal International*, *185*(3), 1417–1430. https://doi.org/10.1111/j.1365-246X.2011.05018.x

Davaille, A. (1999). Simultaneous generation of hotspots and superwells by convection in a heterogeneous planetary mantle. *Nature*, *402*(6763), 756–760. https://doi.org/10.1038/45461

Davidson, A., & Rex, D. C. (1980). Age of volcanism and rifting in southwestern Ethiopia. *Nature*, *283*(5748), 657–658. https://doi.org/10.1038/283657a0

Debayle, E., Lévêque, J. J., & Cara, M. (2001). Seismic evidence for a deeply rooted low-velocity anomaly in the upper mantle beneath the northeastern Afro/Arabian continent. *Earth and Planetary Science Letters*, *193*(3–4), 423–436. https://doi.org/10.1016/S0012-821X(01)00509-X

Dziewonski, A. M., Chou, T. A., & Woodhouse, J. H. (1981). Determination of earthquake source parameters from waveform data for studies of global and regional seismicity. *Journal of Geophysical Research*, *86*(B4), 2825–2852. https://doi.org/10.1029/JB086iB04p02825

Ebinger, C. J., & Casey, M. (2001). Continental breakup in magmatic provinces: An Ethiopian example. *Geology*, *29*(6), 527–530. https://doi.org/10.1130/0091-7613(2001)029<0527:CBIMPA>2.0.CO;2

Ebinger, C. J., Forsyth, D. W., Bow, C. O., & Bowin, C. O. (1989). Effective elastic plate thickness beneath the East African and Afar plateaus and dynamic compensation of the uplifts. *Journal of Geophysical Research*, *94*(B3), 2883–2901. https://doi.org/10.1029/jb094ib03p02883

Ebinger, C. J., Keir, D., Ayele, A., Calais, E., Wright, T. J., Belachew, M., et al. (2008). Capturing magma intrusion and faulting processes during continental rupture: Seismicity of the Dabbahu (Afar) rift. *Geophysical Journal International*, *174*(3), 1138–1152. https://doi.org/10.1111/j.1365-246X.2008.03877.x

Ebinger, C. J., & Sleep, N. H. (1998). Cenozoic magmatism throughout east Africa resulting from impact of a single plume. *Nature*, *395*(October), 788–791. https://doi.org/10.1038/27417

Ebinger, C. J., Yemane, T., Woldegabriel, G., Aronson, J. L., & Walter, R. C. (1993). Late Eocene-Recent volcanism and faulting in the southern main Ethiopian rift. *Journal of the Geological Society*, *150*(1), 99–108. https://doi.org/10.1144/gsjgs.150.1.0099

Ekström, G., Nettles, M., & Dziewoński, A. M. (2012). The global CMT project 2004-2010: Centroid-moment tensors for 13,017 earthquakes. *Physics of the Earth and Planetary Interiors*, *200–201*, 1–9. https://doi.org/10.1016/j.pepi.2012.04.002

Emry, E. L., Shen, Y., Nyblade, A. A., Flinders, A., & Bao, X. (2019). Upper mantle Earth structure in Africa from full-wave ambient noise tomography. *Geochemistry, Geophysics, Geosystems*, *20*(1), 120–147. https://doi.org/10.1029/2018GC007804

Evangelidis, C. P., & Melis, N. S. (2012). Ambient noise levels in Greece as recorded at the Hellenic Unified Seismic Network. *Bulletin of the Seismological Society of America*, *102*(6), 2507–2517. https://doi.org/10.1785/0120110319

Faccenna, C., Becker, T. W., Jolivet, L., & Keskin, M. (2013). Mantle convection in the Middle East: Reconciling Afar upwelling, Arabia indentation and Aegean trench rollback. *Earth and Planetary Science Letters*, *375*, 254–269. https://doi.org/10.1016/j.epsl.2013.05.043

Farnetani, C. G., & Samuel, H. (2005). Beyond the thermal plume paradigm. *Geophysical Research Letters*, *32*(7), 1–4. https://doi.org/10.1029/2005GL022360

Ferguson, D. J., MacLennan, J., Bastow, I. D., Pyle, D. M., Jones, S. M., Keir, D., et al. (2013). Melting during late-stage rifting in Afar is hot and deep. *Nature*, *499*(7456), 70–73. https://doi.org/10.1038/nature12292

Fishwick, S. (2010). Surface wave tomography: Imaging of the lithosphere-asthenosphere boundary beneath central and southern Africa? *Lithos*, *120*(1–2), 63–73. https://doi.org/10.1016/j.lithos.2010.05.011

Fishwick, S., & Bastow, I. D. (2011). Towards a better understanding of African topography: A review of passive-source seismic studies of the African crust and upper mantle. *Geological Society – Special Publications*, *357*(1), 343–371. https://doi.org/10.1144/SP357.19

Foulger, G. R. (2007). The "plate" model for the genesis melting anomalies. *Special Paper 430: Plates, Plumes and Planetary Processes*, 1–28. https://doi.org/10.1130/2007.2430(01)

French, S. W., & Romanowicz, B. A. (2014). Whole-mantle radially anisotropic shear velocity structure from spectral-element waveform tomography. *Geophysical Journal International*, *199*(3), 1303–1327. https://doi.org/10.1093/gji/ggu334

Friederich, W., & Meier, T. (2008). Temporary seismic broadband network Acquired data on Hellenic subduction zone. *Eos, Transactions American Geophysical Union*, *89*(40), 378. https://doi.org/10.1029/2008eo400002

Fullea, J., Lebedev, S., Martinec, Z., & Celli, N. L. (2021). WINTERC-Grav: Mapping the upper mantle thermochemical heterogeneity from coupled geophysical-petrological inversion of seismic waveforms, heat flow, surface elevation and gravity satellite data. *Geophysical Journal International*, *226*(1), 146–191. https://doi.org/10.1093/gji/ggab094

Furman, T., Kaleta, K. M., Bryce, J. G., & Hanan, B. B. (2006). Tertiary mafic lavas of Turkana, Kenya: Constraints on East African plume structure and the occurrence of high-μ volcanism in Africa. *Journal of Petrology*, *47*(6), 1221–1244. https://doi.org/10.1093/petrology/egl009

Gao, S. S., Liu, K. H., & Abdelsalam, M. G. (2010). Seismic anisotropy beneath the Afar Depression and adjacent areas: Implications for mantle flow. *Journal of Geophysical Research*, *115*(12), 1–15. https://doi.org/10.1029/2009JB007141

George, R., & Rogers, N. W. (2002). Plume dynamics beneath the African plate inferred from the geochemistry of the Tertiary basalts of southern Ethiopia. *Contributions to Mineralogy and Petrology*, *144*(3), 286–304. https://doi.org/10.1007/s00410-002-0396-z

George, R., Rogers, N. W., & Kelley, S. P. (1998). Earliest magmatism in Ethiopia: Evidence for two mantle plumes in one flood basalt province. *Geology*, *26*(10), 923–926. https://doi.org/10.1130/0091-7613(1998)026<0923:EMIEEF>2.3.CO;2

Hammond, J. O. S., Kendall, J. M., Stuart, G. W., Ebinger, C. J., Bastow, I. D., Keir, D., et al. (2013). Mantle upwelling and initiation of rift segmentation beneath the Afar Depression. *Geology*, *41*(6), 635–638. https://doi.org/10.1130/G33925.1

Hammond, J. O. S., Kendall, J. M., Stuart, G. W., Keir, D., Ebinger, C., Ayele, A., & Belachew, M. (2011). The nature of the crust beneath the Afar triple junction: Evidence from receiver functions. *Geochemistry, Geophysics, Geosystems*, *12*(12), Q12004. https://doi.org/10.1029/2011GC003738

Hansen, S. E., Nyblade, A. A., & Benoit, M. H. (2012). Mantle structure beneath Africa and Arabia from adaptively parameterized P-wave tomography: Implications for the origin of Cenozoic Afro-Arabian tectonism. *Earth and Planetary Science Letters*, *319–320*, 23–34. https://doi.org/10.1016/j.epsl.2011.12.023

Hendrie, D. B., Kusznir, N. J., Morley, C. K., & Ebinger, C. J. (1994). Cenozoic extension in northern Kenya: A quantitative model of rift basin development in the Turkana region. *Tectonophysics*, *236*(1–4), 409–438. https://doi.org/10.1016/0040-1951(94)90187-2

Heyn, B. H., & Conrad, C. P. (2022). On the relation between basal erosion of the lithosphere and surface heat flux for continental plume tracks. *Geophysical Research Letters*, *49*(7), e2022GL098003. https://doi.org/10.1029/2022GL098003

Kaviani, A., Sandvol, E., Moradi, A., Rümpker, G., Tang, Z., & Mai, P. M. (2018). Mantle transition zone thickness beneath the Middle East: Evidence for segmented Tethyan slabs, delaminated lithosphere, and lower mantle upwelling. *Journal of Geophysical Research: Solid Earth*, *123*(6), 4886–4905. https://doi.org/10.1029/2018JB015627

Keir, D., Hamling, I. J., Ayele, A., Calais, E., Ebinger, C., Wright, T. J., et al. (2009). Evidence for focused magmatic accretion at segment centers from lateral dike injections captured beneath the Red Sea rift in Afar. *Geology*, *37*(1), 59–62. https://doi.org/10.1130/G25147A.1

Kendall, J. M., Pilidou, S., Keir, D., Bastow, I. D., Stuart, G. W., & Ayele, A. (2006). Mantle upwellings, melt migration and the rifting of Africa: Insights from seismic anisotropy. In *Geological society special publication* (Vol. *259*, pp. 55–72). https://doi.org/10.1144/GSL.SP.2006.259.01.06

Kendall, J. M., Stuart, G. W., Ebinger, C. J., Bastow, I. D., & Keir, D. (2005). Magma-assisted rifting in Ethiopia. *Nature*, *433*(7022), 146–148. https://doi.org/10.1038/nature03161

Kieffer, B., Arndt, N., Lapierre, H., Bastien, F., Bosch, D., Pecher, A., et al. (2004). Flood and shield basalts from Ethiopia: Magmas from the African superswell. *Journal of Petrology*, *45*(4), 793–834. https://doi.org/10.1093/petrology/egg112

Koppers, A. A. P., Becker, T. W., Jackson, M. G., Konrad, K., Müller, R. D., Romanowicz, B., et al. (2021). Mantle plumes and their role in Earth processes. *Nature Reviews Earth & Environment*, *2*(6), 382–401. https://doi.org/10.1038/s43017-021-00168-6

Koptev, A., Burov, E., Gerya, T., Le Pourhiet, L., Leroy, S., Calais, E., & Jolivet, L. (2018). Plume-induced continental rifting and break-up in ultra-slow extension context: Insights from 3D numerical modeling. *Tectonophysics*, *746*, 121–137. https://doi.org/10.1016/j.tecto.2017.03.025

Koptev, A., Cloetingh, S., Burov, E., François, T., & Gerya, T. (2017). Long-distance impact of Iceland plume on Norway's rifted margin. *Scientific Reports*, *7*(1), 1–11. https://doi.org/10.1038/s41598-017-07523-y

Koulakov, I., Burov, E., Cloetingh, S., El Khrepy, S., Al Arifi, N., & Bushenkova, N. (2016). Evidence for anomalous mantle upwelling beneath the Arabian Platform from travel time tomography inversion. *Tectonophysics*, *667*, 176–188. https://doi.org/10.1016/j.tecto.2015.11.022

Krienitz, M. S., Haase, K. M., Mezger, K., Van Den Bogaard, P., Thiemann, V., & Shaikh-Mashail, M. A. (2009). Tectonic events, continental intraplate volcanism, and mantle plume activity in northern Arabia: Constraints from geochemistry and Ar-Ar dating of Syrian lavas. *Geochemistry, Geophysics, Geosystems*, *10*(4), Q04008. https://doi.org/10.1029/2008gc002254

Lebedev, S., Bonadio, R., Tsekhmistrenko, M., de Laat, J. I., & Bean, C. J. (2021). Seafloor seismometers look for clues to North Atlantic volcanism. *Eos*, 102. https://doi.org/10.1029/2021EO159380

Lebedev, S., Chevrot, S., & van der Hilst, R. D. (2003). Correlation between the shear-speed structure and thickness of the mantle transition zone. *Physics of the Earth and Planetary Interiors*, *136*(1–2), 25–40. https://doi.org/10.1016/S0031-9201(03)00020-7

Lebedev, S., Nolet, G., Meier, T., & van der Hilst, R. D. (2005). Automated multimode inversion of surface and S waveforms. *Geophysical Journal International*, *162*(3), 951–964. https://doi.org/10.1111/j.1365-246X.2005.02708.x

Lebedev, S., Schaeffer, A. J., Fullea, J., & Pease, V. (2018). Seismic tomography of the arctic region: Inferences for the thermal structure and evolution of the lithosphere. *Geological Society – Special Publications*, *460*(1), 419–440. https://doi.org/10.1144/sp460.10

Lebedev, S., & Van Der Hilst, R. D. (2008). Global upper-mantle tomography with the automated multimode inversion of surface and S-wave forms. *Geophysical Journal International*, *173*(2), 505–518. https://doi.org/10.1111/j.1365-246X.2008.03721.x

Lees, M. E., Rudge, J. F., & McKenzie, D. (2020). Gravity, topography, and melt generation rates from simple 3-D models of mantle convection. *Geochemistry, Geophysics, Geosystems*, *21*(4), e2019GC008809. https://doi.org/10.1029/2019GC008809

Legendre, C. P., Meier, T., Lebedev, S., Friederich, W., & Viereck-Götte, L. (2012). A shear wave velocity model of the European upper mantle from automated inversion of seismic shear and surface waveforms. *Geophysical Journal International*, *191*(1), 282–304. https://doi.org/10.1111/j.1365-246X.2012.05613.x

Leroy, S., Lucazeau, F., Razin, P., & Manatschal, G., & YOCMAL Team. (2007). Young conjugate margins laboratory in the Gulf of Aden: The YOCMAL project. *AGU Fall Meeting Abstracts*, *2007*, T41A–T0350.

Lim, J. A., Chang, S. J., Mai, P. M., & Zahran, H. (2020). Asthenospheric flow of plume material beneath Arabia inferred from S wave traveltime tomography. *Journal of Geophysical Research: Solid Earth*, *125*(8). https://doi.org/10.1029/2020JB019668

Mackenzie, G. D., Thybo, H., & Maguire, P. K. H. (2005). Crustal velocity structure across the Main Ethiopian Rift: Results from two-dimensional wide-angle seismic modelling. *Geophysical Journal International*, *162*(3), 994–1006. https://doi.org/10.1111/j.1365-246X.2005.02710.x

Maguire, P. K. H., Ebinger, C. J., Stuart, G. W., Mackenzie, G. D., Whaler, K. A., Kendall, J. M., et al. (2003). Geophysical project in Ethiopia studies continental breakup. *EOS*, *84*(35), 3–8. https://doi.org/10.1029/2003EO350002

Mcguire, A. V., & Bohannon, R. G. (1989). Timing of mantle upwelling: Evidence for a passive origin for the Red Sea rift. *Journal of Geophysical Research*, *94*(B2), 1677–1682. https://doi.org/10.1029/JB094iB02p01677

Mechie, J., Abu-Ayyash, K., Ben-Avraham, Z., El-Kelani, R., Mohsen, A., Rümpker, G., et al. (2005). Crustal shear velocity structure across the Dead Sea Transform from two-dimensional modelling of DESERT project explosion seismic data. *Geophysical Journal International*, *160*(3), 910–924. https://doi.org/10.1111/j.1365-246X.2005.02526.x

Mechie, J., Abu-Ayyash, K., Ben-Avraham, Z., El-Kelani, R., Qabbani, I., Weber, M., et al. (2009). Crustal structure of the southern Dead Sea basin derived from project DESIRE wide-angle seismic data. *Geophysical Journal International*, *178*(1), 457–478. https://doi.org/10.1111/j.1365-246X.2009.04161.x

Mohsen, A., Kind, R., Sobolev, S. V., & Weber, M. (2006). Thickness of the lithosphere east of the Dead Sea Transform. *Geophysical Journal International*, *167*(2), 845–852. https://doi.org/10.1111/j.1365-246X.2006.03185.x

Montagner, J. P., Marty, B., Stutzmann, E., Sicilia, D., Cara, M., Pik, R., et al. (2007). Mantle upwellings and convective instabilities revealed by seismic tomography and helium isotope geochemistry beneath eastern Africa. *Geophysical Research Letters*, *34*(21), 1–6. https://doi.org/10.1029/2007GL031098

Montelli, R., Nolet, G., Dahlen, F. A., & Masters, G. (2006). A catalogue of deep mantle plumes: New results from finite frequency tomography. *Geochemistry, Geophysics, Geosystems*, *7*(11), Q11007. https://doi.org/10.1029/2006gc001248

Morgan, W. J. (1971). Convection plumes in the lower mantle. *Nature*, *230*(5), 42–43. https://doi.org/10.1038/230042a0

Morgan, W. J. (1972). Plate motions and deep mantle convection. *Memoirs – Geological Society of America*, *132*(3), 7–22. https://doi.org/10.1130/MEM132-p7

Mulibo, G. D., & Nyblade, A. A. (2013). Mantle transition zone thinning beneath eastern Africa: Evidence for a whole-mantle superplume structure. *Geophysical Research Letters*, *40*(14), 3562–3566. https://doi.org/10.1002/grl.50694

Nelson, W. R., Furman, T., van Keken, P. E., Shirey, S. B., & Hanan, B. B. (2012). OsHf isotopic insight into mantle plume dynamics beneath the East African Rift System. *Chemical Geology*, *320–321*, 66–79. https://doi.org/10.1016/j.chemgeo.2012.05.020

Nolet, G. (1990). Partitioned waveform inversion and two-dimensional structure under the network of autonomously recording seismographs. *Journal of Geophysical Research*, *95*(B6), 8499–8512. https://doi.org/10.1029/JB095iB06p08499

Nyblade, A. A., Birt, C., Langston, C. A., Owens, T. J., & Last, R. J. (1996). Seismic experiment reveals rifting of craton in Tanzania. *Eos*, *77*(51), 517. https://doi.org/10.1029/96EO00339

Nyblade, A. A., Dirks, P., Graham, G., Webb, S., Jones, M., & Cooper, G. (2008). AfricaArray: Developing a geosciences workforce for Africa's natural resource sector. *The Leading Edge*, *27*(10), 1358–1361. https://doi.org/10.3109/09638239209005451

Nyblade, A. A., Durrheim, R., Dirks, P., Graham, G., Gibson, R., & Webb, S. (2011). Geoscience Initiative develops sustainable science in Africa. *Eos*, *92*(19), 161–162. https://doi.org/10.1029/2011EO190002

Nyblade, A. A., & Langston, C. A. (2002). Broadband seismic experiments probe the East African rift. *Eos*, *83*(37), 405–409. https://doi.org/10.1029/2002EO000296

Nyblade, A. A., & Robinson, S. W. (1994). The African superswell. *Geophysical Research Letters*, *21*(9), 765–768. https://doi.org/10.1029/94gl00631

Park, Y., & Nyblade, A. A. (2006). P-wave tomography reveals a westward dipping low velocity zone beneath the Kenya Rift. *Geophysical Research Letters*, *33*(7), 1–4. https://doi.org/10.1029/2005GL025605

Paul, A., Hatzfeld, D., Karabulut, H., Hatzidimitriou, P., Childs, D. M., Nikolova, S., et al. (2008). The SIMBAAD experiment in W-Turkey and Greece: A dense seismic network to study the crustal and mantle structures. *AGU Fall Meeting Abstracts*, *2008*, T21A–T1926.

Peace, A. L., Phethean, J. J. J., Franke, D., Foulger, G. R., Schiffer, C., Welford, J. K., et al. (2020). A review of Pangaea dispersal and Large Igneous Provinces – In search of a causative mechanism. *Earth-Science Reviews*, *206*, 102902. https://doi.org/10.1016/j.earscirev.2019.102902

Pik, R., Marty, B., & Hilton, D. R. (2006). How many mantle plumes in Africa? The geochemical point of view. *Chemical Geology*, *226*(3–4), 100–114. https://doi.org/10.1016/j.chemgeo.2005.09.016

Pitilakis, K., Karapetrou, S., Bindi, D., Manakou, M., Petrovic, B., Roumelioti, Z., et al. (2016). Structural monitoring and earthquake early warning systems for the AHEPA hospital in Thessaloniki. *Bulletin of Earthquake Engineering*, *14*(9), 2543–2563. https://doi.org/10.1007/s10518-016-9916-5

Qaysi, S., Liu, K. H., & Gao, S. S. (2018). A database of shear-wave splitting measurements for the Arabian plate. *Seismological Research Letters*, *89*(6), 2294–2298. https://doi.org/10.1785/0220180144

Rawlinson, N., & Spakman, W. (2016). On the use of sensitivity tests in seismic tomography. *Geophysical Journal International*, *205*(2), 1221–1243. https://doi.org/10.1093/gji/ggw084

Richards, M. A., Duncan, R. A., & Courtillot, V. E. (1989). Flood basalts and hot spot tracks: Plumes heads and tails. *Science*, *246*(10), 103–107. https://doi.org/10.1126/science.246.4926.103

Rickers, F., Fichtner, A., & Trampert, J. (2013). The Iceland-Jan Mayen plume system and its impact on mantle dynamics in the North Atlantic region: Evidence from full-waveform inversion. *Earth and Planetary Science Letters*, *367*, 39–51. https://doi.org/10.1016/j.epsl.2013.02.022

Ritsema, J., Van Heijst, H. J., & Woodhouse, J. H. (1999). Complex shear wave velocity structure imaged beneath Africa and Iceland. *Science*, *286*(5446), 1925–1931. https://doi.org/10.1126/science.286.5446.1925

Rodgers, A., Harris, D., Ruppert, S., Lewis, J. P., O'Boyle, J., Pasyanos, M., et al. (2003). A broadband seismic deployment in Jordan. *Seismological Research Letters*, *74*(4), 374–381. https://doi.org/10.1785/gssrl.74.4.374

Rogers, N. W. (2006). Basaltic magmatism and the geodynamics of the East African Rift System. *Geological Society Special Publication*, *259*, 77–93. https://doi.org/10.1144/GSL.SP.2006.259.01.08

Rooney, T. O. (2010). Geochemical evidence of lithospheric thinning in the southern Main Ethiopian Rift. *Lithos*, *117*(1–4), 33–48. https://doi.org/10.1016/j.lithos.2010.02.002

Rooney, T. O. (2017). The Cenozoic magmatism of East-Africa: Part I — Flood basalts and pulsed magmatism. *Lithos*, *286–287*, 264–301. https://doi.org/10.1016/j.lithos.2017.05.014

Rooney, T. O. (2020a). The Cenozoic magmatism of East Africa: Part II – Rifting of the mobile belt. *Lithos*, *360–361*, 105291. https://doi.org/10.1016/j.lithos.2019.105291

Rooney, T. O. (2020b). The Cenozoic magmatism of East Africa: Part V – Magma sources and processes in the East African rift. *Lithos*, *360–361*, 105296. https://doi.org/10.1016/j.lithos.2019.105296

Rooney, T. O., Furman, T., Yirgu, G., & Ayalew, D. (2005). Structure of the Ethiopian lithosphere: Xenolith evidence in the main Ethiopian rift. *Geochimica et Cosmochimica Acta*, *69*(15), 3889–3910. https://doi.org/10.1016/j.gca.2005.03.043

Rooney, T. O., Herzberg, C., & Bastow, I. D. (2012). Elevated mantle temperature beneath East Africa. *Geology*, *40*(1), 27–30. https://doi.org/10.1130/G32382.1

Rychert, C. A., Hammond, J. O. S., Harmon, N., Michael Kendall, J., Keir, D., Ebinger, C., et al. (2012). Volcanism in the Afar Rift sustained by decompression melting with minimal plume influence. *Nature Geoscience*, *5*(6), 406–409. https://doi.org/10.1038/ngeo1455

Sandvol, E., Al-Damegh, K., Calvert, A., Seber, D., Barazangi, M., Mohamad, R., et al. (2001). Tomographic imaging of Lg and Sn propagation in the Middle East. *Pure and Applied Geophysics*, *158*(7), 1121–1163. https://doi.org/10.1007/978-3-0348-8262-0_3

Sandvol, E., Seber, D., Barazangi, M., Vernon, F. L., Mellors, R., & Al-amri, A. M. (1998). Lithospheric seismic velocity discontinuities beneath the Arabian Shield. *Geophysical Research Letters*, *25*(15), 2873–2876. https://doi.org/10.1029/98gl02214

Sandvol, E., Turkelli, N., & Barazangi, M. (2003). The Eastern Turkey Seismic Experiment: The study of a young continent-continent collision. *Geophysical Research Letters*, *30*(24), 1–2. https://doi.org/10.1029/2003GL018912

Schaeffer, A. J., & Lebedev, S. (2013). Global shear speed structure of the upper mantle and transition zone. *Geophysical Journal International*, *194*(1), 417–449. https://doi.org/10.1093/gji/ggt095

Schaeffer, A. J., & Lebedev, S. (2014). Imaging the North American continent using waveform inversion of global and USArray data. *Earth and Planetary Science Letters*, *402*(C), 26–41. https://doi.org/10.1016/j.epsl.2014.05.014

Schoonman, C. M., White, N. J., & Pritchard, D. (2017). Radial viscous fingering of hot asthenosphere within the Icelandic plume beneath the North Atlantic Ocean. *Earth and Planetary Science Letters*, *468*, 51–61. https://doi.org/10.1016/j.epsl.2017.03.036

Sebai, A., Stutzmann, E., Montagner, J. P., Sicilia, D., & Beucler, E. (2006). Anisotropic structure of the African upper mantle from Rayleigh and Love wave tomography. *Physics of the Earth and Planetary Interiors*, *155*(1–2), 48–62. https://doi.org/10.1016/j.pepi.2005.09.009

Şengör, A. M. C., Özeren, S., Genç, T., & Zor, E. (2003). East Anatolian High Plateau as a mantle-supported, north-south shortened domal structure. *Geophysical Research Letters*, *30*(24), 2–5. https://doi.org/10.1029/2003GL017858

Sicilia, D., Montagner, J. P., Cara, M., Stutzmann, E., Debayle, E., Lépine, J. C., et al. (2008). Upper mantle structure of shear-waves velocities and stratification of anisotropy in the Afar Hotspot region. *Tectonophysics*, *462*(1–4), 164–177. https://doi.org/10.1016/j.tecto.2008.02.016

Silver, P., Mainprice, D., Ismaïl, W., Tommasi, A., Silver, P., Mainprice, D., et al. (2016). Mantle structural geology from seismic anisotropy. In *Mantle petrology: Field observations and high pressure experimentations: A tribute to Francis R. (Joe) Boyd* (Vol. 6). The Geochemical Society.

Silver, P. G., Russo, R. M., & Lithgow-bertelloni, C. (1998). Coupling of South American and African plate motion and plate deformation. *Science*, *279*(5347), 60–63. https://doi.org/10.1126/science.279.5347.60

Sleep, N. H. (1997). Lateral flow and ponding of starting plume material. *Journal of Geophysical Research*, *102*(B5), 10001–10012. https://doi.org/10.1029/97jb00551

Sobolev, S. V., Sobolev, A. V., Kuzmin, D. V., Krivolutskaya, N. A., Petrunin, A. G., Arndt, N. T., et al. (2011). Linking mantle plumes, large igneous provinces and environmental catastrophes. *Nature*, *477*(7364), 312–316. https://doi.org/10.1038/nature10385

Steinberger, B., Bredow, E., Lebedev, S., Schaeffer, A., & Torsvik, T. H. (2019). Widespread volcanism in the Greenland–North Atlantic region explained by the Iceland plume. *Nature Geoscience*, *12*(1), 61–68. https://doi.org/10.1038/s41561-018-0251-0

Stern, R. J., & Johnson, P. (2010). Continental lithosphere of the Arabian Plate: A geologic, petrologic, and geophysical synthesis. *Earth-Science Reviews*, *101*(1–2), 29–67. https://doi.org/10.1016/j.earscirev.2010.01.002

Stuart, G., Kendall, M., Bastow, I., Ayele, A., Ebinger, C., Maguire, P., & Fowler, M. (2002). The EAGLE broadband seismic experiment – A study of continental rifting in the Ethiopia. In *AGU Fall Meeting Abstracts* (Vol. *2002*, pp. T11D–T1289).

Sun, M., Liu, K. H., Fu, X., & Gao, S. S. (2017). Receiver function imaging of mantle transition zone discontinuities beneath the Tanzania craton and adjacent segments of the East African Rift System. *Geophysical Research Letters*, *44*(24), 116–124. https://doi.org/10.1002/2017gl075485

Tang, Z., Mai, P. M., Chang, S. J., & Zahran, H. (2018). Evidence for crustal low shear-wave speed in Western Saudi Arabia from multi-scale fundamental-mode Rayleigh-wave group-velocity tomography. *Earth and Planetary Science Letters*, *495*, 24–37. https://doi.org/10.1016/j.epsl.2018.05.011

Thompson, D. A., Hammond, J. O. S., Kendall, J.-M., Stuart, G. W., Helffrich, G. R., Keir, D., et al. (2015). Hydrous upwelling across the mantle transition zone beneath the Afar Triple Junction. *Geochemistry, Geophysics, Geosystems*, *16*(3), 834–846. https://doi.org/10.1002/2014GC005648

Torsvik, T. H., Steinberger, B., Shephard, G. E., Doubrovine, P. V., Gaina, C., Domeier, M., et al. (2019). Pacific-Panthalassic reconstructions: Overview, errata and the way forward. *Geochemistry, Geophysics, Geosystems*, *20*(7), 3659–3689. https://doi.org/10.1029/2019GC008402

Tsekhmistrenko, M., Sigloch, K., Hosseini, K., & Barruol, G. (2021). A tree of Indo-African mantle plumes imaged by seismic tomography. *Nature Geoscience*, *14*(8), 612–619. https://doi.org/10.1038/s41561-021-00762-9

Tumanova, N., Kakhoberashvili, S., Omarashvili, V., Tserodze, M., & Akubardia, D. (2016). National seismic network of Georgia. *AGU Fall Meeting Abstracts*, *2016*, S11D–S2498.

van der Meer, D. G., van Hinsbergen, D. J. J., & Spakman, W. (2018). Atlas of the underworld: Slab remnants in the mantle, their sinking history, and a new outlook on lower mantle viscosity. *Tectonophysics*, *723*, 309–448. https://doi.org/10.1016/j.tecto.2017.10.004

Vicente de Gouveia, S., Besse, J., Frizon de Lamotte, D., Greff-Lefftz, M., Lescanne, M., Gueydan, F., & Leparmentier, F. (2018). Evidence of hotspot paths below Arabia and the horn of Africa and consequences on the Red Sea opening. *Earth and Planetary Science Letters*, *487*, 210–220. https://doi.org/10.1016/j.epsl.2018.01.030

Wang, Z., & Dahlen, F. A. (1995). Spherical-spline parameterization of three-dimensional Earth models. *Geophysical Research Letters*, *22*(22), 3099–3102. https://doi.org/10.1029/95gl03080

Wessel, P., Smith, W. H. F., Scharroo, R., Luis, J., & Wobbe, F. (2013). Generic mapping tools: Improved version released. *EOS*, *94*(45), 409–410. https://doi.org/10.1002/2013EO450001

10.1029/2022GC010610

White, N., & Lovell, B. (1997). Measuring the pulse of a plume with the sedimentary record. *Nature*, *387*(6636), 888–891. https://doi.org/10.1038/43151

White, R., & McKenzie, D. (1989). Magmatism at rift zones: The generation of volcanic continental margins and flood basalts. *Journal of Geophysical Research*, *94*(B6), 7685–7729. https://doi.org/10.1029/JB094iB06p07685

Wolfenden, E., Ebinger, C., Yirgu, G., Deino, A., & Ayalew, D. (2004). Evolution of the northern Main Ethiopian rift: Birth of a triple junction. *Earth and Planetary Science Letters*, *224*(1–2), 213–228. https://doi.org/10.1016/j.epsl.2004.04.022

Wolfenden, E., Ebinger, C., Yirgu, G., Renne, P. R., & Kelley, S. P. (2005). Evolution of a volcanic rifted margin: Southern Red Sea, Ethiopia. *Bulletin of the Geological Society of America*, *117*(7–8), 846–864. https://doi.org/10.1130/B25516.1

Yao, Z., Mooney, W. D., Zahran, H. M., & Youssef, S. E. H. (2017). Upper mantle velocity structure beneath the Arabian shield from Rayleigh surface wave tomography and its implications. *Journal of Geophysical Research: Solid Earth*, *122*(8), 6552–6568. https://doi.org/10.1002/2016JB013805

References From the Supporting Information

Aldanmaz, E., Pearce, J. A., Thirlwall, M. F., & Mitchell, J. G. (2000). Petrogenetic evolution of late Cenozoic, post-collision volcanism in Western Anatolia, Turkey. *Journal of Volcanology and Geothermal Research*, *102*(1–2), 67–95. https://doi.org/10.1016/S0377-0273(00)00182-7

Argus, D. F., Gordon, R. G., & Demets, C. (2011). Geologically current motion of 56 plates relative to the no-net-rotation reference frame. *Geochemistry, Geophysics, Geosystems*, *12*(11), 1–13. https://doi.org/10.1029/2011GC003751

Baker, B. H. (1986). Tectonics and volcanism of the southern Kenya Rift Valley and its influence on rift sedimentation. *Geological Society – Special Publications*, *25*(25), 45–57. https://doi.org/10.1144/GSL.SP.1986.025.01.05

Baldridge, W. S., Eyal, Y., Bartov, Y., Steinitz, G., & Eyal, M. (1991). Miocene magmatism of Sinai related to the opening of the red sea. *Tectonophysics*, *197*(2–4), 181–201. https://doi.org/10.1016/0040-1951(91)90040-Y

Bartol, J., & Govers, R. (2014). A single cause for uplift of the Central and Eastern Anatolian plateau? *Tectonophysics*, *637*, 116–136. https://doi.org/10.1016/j.tecto.2014.10.002

Camp, V. E., Hooper, P. R., Roobol, M. J., & White, D. L. (1987). The Madinah eruption, Saudi Arabia: Magma mixing and simultaneous extrusion of three basaltic chemical types. *Bulletin of Volcanology*, *49*(2), 680–693. https://doi.org/10.1007/bf01245475

Camp, V. E., Roobol, M. J., & Hooper, P. R. (1989). The Arabian continental alkali basalt province: Part III. Evolution of Harrat Kishb, Kingdom of Saudi Arabia. *The Geological Society of America Bulletin*, *104*(4), 379–396. https://doi.org/10.1130/0016-7606(1992)104<0379:TACABP>2.3.CO;2

Camp, V. E., Roobol, M. J., & Hooper, P. R. (1991). The Arabian continental alkali basalt province: Part II. Evolution of Harrats Khaybar, Ithnayn, and Kura, Kingdom of Saudi Arabia. *The Geological Society of America Bulletin*, *103*(3), 363–391. https://doi.org/10.1130/0016-7606(1992)104<0379:TACABP>2.3.CO;2

Deniel, C., Vidal, P., Coulon, C., Vellutini, P. J., & Piguet, P. (1994). Temporal evolution of mantle sources during continental rifting: The volcanism of Djibouti (Afar). *Journal of Geophysical Research*, *99*(B2), 2853–2869. https://doi.org/10.1029/93JB02576

Dilek, Y., & Whitney, D. L. (2000). Cenozoic crustal evolution in Central Anatolia: Extension, magmatism and landscape development. In *Proceedings of the Third International Conference on the Geology of the Eastern Mediterranean* (pp. 183–192).

Doubrovine, P. V., Steinberger, B., & Torsvik, T. H. (2012). Absolute plate motions in a reference frame defined by moving hot spots in the Pacific, Atlantic, and Indian oceans. *Journal of Geophysical Research*, *117*(9), 1–30. https://doi.org/10.1029/2011JB009072

Doubrovine, P. V., Steinberger, B., & Torsvik, T. H. (2016). A failure to reject: Testing the correlation between large igneous provinces and deep mantle structures with EDF statistics. *Geochemistry, Geophysics, Geosystems*, *17*(4), 1130–1163. https://doi.org/10.1002/2015GC006205

Ercan, T., Satir, M., Stenitz, G., Dora, A., Sarifakioglu, E., Adis, C., et al. (1995). Features of the tertiary volcanism observed at Biga penisnsula and Gökçeada, Tavsan Islands. *Bulletin of the Mineral Research and Exploration*, *117*, 55–86.

Ershov, A. V., & Nikishin, A. M. (2004). Recent geodynamics of the Caucasus-Arabia-East Africa region. *Geotectonics*, *38*(2), 123–136.

Furman, T., Bryce, J. G., Karson, J., & Iotti, A. (2004). East African Rift System (EARS) plume structure: Insights from quaternary mafic lavas of Turkana, Kenya. *Journal of Petrology*, *45*(5), 1069–1088. https://doi.org/10.1093/petrology/egh004

Hofmann, C., Courtillot, V., Féraud, G., Rochette, P., Yirgu, G., & Pik, R. (1997). Timing of the Ethiopian flood basalt event and implications for plume birth and global change. *Nature*, *246*(5429), 170–841. https://doi.org/10.1038/246170a0

Hosseini, K., Matthews, K. J., Sigloch, K., Shephard, G. E., Domeier, M., & Tsekhmistrenko, M. (2018). SubMachine: Web-based tools for exploring seismic tomography and other models of Earth's deep interior. *Geochemistry, Geophysics, Geosystems*, *19*(5), 1464–1483. https://doi.org/10.1029/2018GC007431

Ilani, S., Harlavan, Y., Tarawneh, K., Rabba, I., Weinberger, R., Ibrahim, K., et al. (2001). New K-Ar ages of basalts from the Harrat Ash Shaam volcanic field in Jordan: Implications for the span and duration of the upper-mantle upwelling beneath the Western Arabian plate. *Geology*, *29*(2), 171–174. https://doi.org/10.1130/0091-7613(2001)029<0171:NKAAOB>2.0.CO;2

Innocenti, F., Agostini, S., Di Vincenzo, G., Doglioni, C., Manetti, P., Savaşçin, M. Y., & Tonarini, S. (2005). Neogene and Quaternary volcanism in Western Anatolia: Magma sources and geodynamic evolution. *Marine Geology*, *221*(1–4), 397–421. https://doi.org/10.1016/j.margeo.2005.03.016

Keskin, M., Pearce, J. A., & Mitchell, J. G. (1998). Volcano-stratigraphy and geochemistry of collision-related volcanism on the Erzurum-Kars Plateau, northeastern Turkey. *Journal of Volcanology and Geothermal Research*, *85*(1–4), 355–404. https://doi.org/10.1016/S0377-0273(98)00063-8

Lahitte, P., Gillot, P. Y., & Courtillot, V. (2003). Silicic central volcanoes as precursors to rift propagation: The Afar case. *Earth and Planetary Science Letters*, *207*(1–4), 103–116. https://doi.org/10.1016/S0012-821X(02)01130-5

Lustrino, M., Keskin, M., Mattioli, M., & Kavak, O. (2012). Heterogeneous mantle sources feeding the volcanic activity of Mt. Karacadaĝ (SE Turkey). *Journal of Asian Earth Sciences*, *46*, 120–139. https://doi.org/10.1016/j.jseaes.2011.11.016

Ma, G. S. K., Malpas, J., Xenophontos, C., & Chan, G. H. N. (2011). Petrogenesis of latest miocene-quaternary continental intraplate volcanism along the northern Dead Sea Fault System (Al Ghab-Homs Volcanic Field), Western Syria: Evidence for lithosphere-asthenosphere interaction. *Journal of Petrology*, *52*(2), 401–430. https://doi.org/10.1093/petrology/egq085

Mana, S., Furman, T., Turrin, B. D., Feigenson, M. D., & Swisher, C. C. (2015). Magmatic activity across the East African North Tanzanian divergence zone. *Journal of the Geological Society*, *172*(3), 368–389. https://doi.org/10.1144/jgs2014-072

Matthews, K. J., Maloney, K. T., Zahirovic, S., Williams, S. E., Seton, M., & Müller, R. D. (2016). Global plate boundary evolution and kinematics since the late Paleozoic. *Global and Planetary Change*, *146*, 226–250. https://doi.org/10.1016/j.gloplacha.2016.10.002

Muller, R. D., Royer, J. Y., & Lawver, L. A. (1993). Revised plate motions relative to the hotspots from combined Atlantic and Indian Ocean hotspot tracks. *Geology*, *21*(3), 275–278. https://doi.org/10.1130/0091-7613(1993)021<0275:RPMRTT>2.3.CO;2

O'Neill, C., Müller, D., & Steinberger, B. (2005). On the uncertainties in hot spot reconstructions and the significance of moving hot spot reference frames. *Geochemistry, Geophysics, Geosystems*, *6*(4), Q04003. https://doi.org/10.1029/2004gc000784
Özdemir, Y., Karaoğlu, Ö., Tolluoğlu, A. Ü., & Güleç, N. (2006). Volcanostratigraphy and petrogenesis of the Nemrut stratovolcano (East Anatolian High Plateau): The most recent post-collisional volcanism in Turkey. *Chemical Geology*, *226*(3–4), 189–211. https://doi.org/10.1016/j.chemgeo.2005.09.020
Pik, R., Deniel, C., Coulon, C., Yirgu, G., & Marty, B. (1999). Isotopic and trace element signatures of Ethiopian flood basalts: Evidence for plume-lithosphere interactions. *Geochimica et Cosmochimica Acta*, *63*(15), 2263–2279. https://doi.org/10.1016/S0016-7037(99)00141-6
Schettino, A., & Scotese, C. R. (2005). Apparent polar wander paths for the major continents (200 Ma to the present day): A palaeomagnetic reference frame for global plate tectonic reconstructions. *Geophysical Journal International*, *163*(2), 727–759. https://doi.org/10.1111/j.1365-246X.2005.02638.x
Schilling, J., Kingsley, R. H., Hanan, B. B., & Mccully, B. L. (1992). Nd-Sr-Pb isotopic variations along the Gulf of Aden' evidence for Afar mantle plume-continental lithosphere interaction. *Journal of Geophysical Research*, *97*(B7), 927–966. https://doi.org/10.1029/92jb00415
Sebai, A., Zumbo, V., Féraud, G., Bertrand, H., Hussain, A. G., Giannérini, G., & Campredon, R. (1991). $^{40}Ar^{39}Ar$ dating of alkaline and tholeiitic magmatism of Saudi Arabia related to the early Red Sea Rifting. *Earth and Planetary Science Letters*, *104*(2–4), 473–487. https://doi.org/10.1016/0012-821X(91)90223-5
Seton, M., Müller, R. D., Zahirovic, S., Gaina, C., Torsvik, T., Shephard, G., et al. (2012). Global continental and ocean basin reconstructions since 200 Ma. *Earth-Science Reviews*, *113*(3–4), 212–270. https://doi.org/10.1016/j.earscirev.2012.03.002
Simmons, N. A., Myers, S. C., Johannesson, G., & Matzel, E. (2012). LLNL-G3Dv3: Global P wave tomography model for improved regional and teleseismic travel time prediction. *Journal of Geophysical Research*, *117*(10), B10302. https://doi.org/10.1029/2012jb009525
Stab, M., Bellahsen, N., Pik, R., Quidelleur, X., Ayalew, D., & Leroy, S. (2016). Modes of rifting in magma-rich settings: Tectono-magmatic evolution of Central Afar. *Tectonics*, *35*(1), 2–38. https://doi.org/10.1002/2015TC003893
Torsvik, T. H., Steinberger, B., Cocks, L. R. M., & Burke, K. (2008). Longitude: Linking Earth's ancient surface to its deep interior. *Earth and Planetary Science Letters*, *276*(3–4), 273–282. https://doi.org/10.1016/j.epsl.2008.09.026
Torsvik, T. H., Van der Voo, R., Preeden, U., Mac Niocaill, C., Steinberger, B., Doubrovine, P. V., et al. (2012). Phanerozoic polar wander, palaeogeography and dynamics. *Earth-Science Reviews*, *114*(3–4), 325–368. https://doi.org/10.1016/j.earscirev.2012.06.007
Van Der Meer, D. G., Spakman, W., Van Hinsbergen, D. J. J., Amaru, M. L., & Torsvik, T. H. (2010). Towards absolute plate motions constrained by lower-mantle slab remnants. *Nature Geoscience*, *3*(1), 36–40. https://doi.org/10.1038/ngeo708
Weinstein, Y., & Garfunkel, Z. (2014). The Dead Sea transform and the volcanism in Northwestern Arabia. *Dead Sea Transform Fault System: Review*, *6*, 91–108. https://doi.org/10.1007/978-94-017-8872-4_4